Received Date : 08-Feb-2016

Revised Date : 03-Oct-2016

Accepted Date : 12-Oct-2016

Article type : Original Article

Jurassic rifting to post-rift subsidence analysis in the Central High Atlas and its relation to salt diapirism

Mar Moragas[a*], Jaume Vergés[a], Eduard Saura[a], Juan-Diego Martín-Martín[a,b], Grégoire Messager[a,f], Óscar Merino-Tomé[c], Isabel Suárez-Ruiz[d], Philippe Razin[e], Carine Grélaud[e], Manon Malaval[e], Rémi Joussiaume[e], David William Hunt[f]

[a] Group of Dynamic of the Lithosphere (GDL), Institute of Earth Sciences Jaume Almera, ICTJA-CSIC, Lluís Solé i Sabarís s/n, 08028 Barcelona, Spain

[b] Departament de Mineralogia, Petrologia i Geologia Aplicada, Universitat de Barcelona (UB), Martí i Franquès s/n, 08028 Barcelona, Spain

[c] Department of Geology, Oviedo University, Jesús Arias de Velasco s/n, 33005 Oviedo, Spain

[d] Instituto Nacional del Carbón (INCAR-CSIC), Francisco Pintado Fe 26, 33011 Oviedo, Spain

[e] EGID Institute, Bordeaux 3 University, Allée Daguin 1, 33607 Pessac Cedex, France

[f] Statoil, TDP RDI CPR CP, Sandsliveiein 90, 5020, Bergen, Norway

*Corresponding author. Present address: Group of Dynamic of the Lithosphere (GDL), Institute of Earth Sciences Jaume Almera, ICTJA-CSIC, Lluís Solé i Sabarís s/n, 08028 Barcelona, Spain. E-mail address: mmoragas@ictja.csic.es

ABSTRACT

The subsidence evolution of the Tethyan Moroccan Atlas Basin, presently inverted as the Central High Atlas, is characterised by an Early Jurassic rifting episode, synchronous with salt diapirism of the Triassic evaporite-bearing rocks. Two contrasting regions of the rift basin - with and without salt diapirism - are examined in order to assess the effect of salt tectonics in the evolution of subsidence patterns and stratigraphy. The Djebel Bou Dahar platform to basin system, located in the southern margin of the Atlas Basin, shows a Lower Jurassic record of normal faulting and lacks any evidence of salt diapirism. In contrast, the Tazoult ridge and adjacent Amezraï basin, located in the centre of the Atlas Basin, reveals spectacular Early Jurassic diapirism. In addition, we analyse alternative Central High Atlas post-Middle Jurassic geohistories based on new thermal and burial models (GENEX® 4.0.3 software), constrained by new vitrinite reflectance data from the Amezraï basin. The comparison of the new subsidence curves from the studied areas with published subsidence curves from the Moroccan Atlas, the Saharan Atlas (Algeria) and Tunisian Atlas show that fast subsidence peaks were diachronous along the strike, being younger towards the east from Early – Middle Jurassic to Late Cretaceous. This analysis also evidences a close relationship between these high subsidence rate episodes and salt diapirism.

Keywords: High Atlas rifting, Thermal model, Subsidence analysis, Geohistory, Atlas diapiric province.

INTRODUCTION

Subsidence patterns of the Atlas Jurassic rift basin that extends from offshore Morocco to Tunisia is extensively reported in the literature (Bracène et al., 2003; Ellouz et al., 2003; Patriat et al., 2003; Zühlke et al., 2004) (Fig.1). However, only a few studies correspond to the Central High Atlas in Morocco (Poisson et al., 1998; Ellouz et al., 2003; Lachkar et al., 2009) and these are mostly localised along the margins of the Atlas Fold Belt abutting stable areas. As such, these studies do not take into consideration the influence of the extensive salt diapirism that is focused towards the centre of the rift basin. This is an important limitation since diapirism in the Central High Atlas has long been acknowledged (Laville, 1988; Bouchouata, 1994; Bouchouata et al., 1995; Ettaki et al., 2007; Ibouh et al., 2011; Michard et al., 2011). Saura et al. (2014), based on integrated structural and stratigraphic work, interpreted the Central High Atlas to represent an extensive diapiric province punctuated by ENE-WSW structural highs representing diapiric walls with the intervening synclines being minibasins that were active during Early and Middle Jurassic times and thus partly synchronous to extensional tectonics.

In this study, we evaluated the subsidence history during the Early and Middle Jurassic within the Central High Atlas of Morocco and the influence of the interaction between both tectonic- and salt-tectonic driven subsidence patterns. We revisited the inverted Atlas rift basin to analyse and compare subsidence curves from different tectonic domains within the basin, i.e. from the fault domain and unstable domain of the rift basin (Fig. 2).

In the fault domain, a system of normal faults and tilted blocks developed and controlled the formation of the carbonate platform and the transition to more basinal settings. In this context we analysed the subsidence evolution of the Djebel Bou Dahar area (Fig. 2), a superbly exposed, well-known and well-constrained example of a Lower Jurassic carbonate platform that developed on top of a basement high controlled and bounded by normal faults

(Verwer et al., 2009; Merino-Tomé et al., 2012). In contrast to the periphery of the Central High Atlas basin, the unstable domain of the basin is characterized by the growth of salt diapiric structures, considered to be partially contemporaneous with the activity of normal faults at depth (Malaval et al., 2014; Saura et al., 2014). To date we have made a detailed and integrated structural and stratigraphic study of 7 salt diapirs in this setting. Of these, the Tazoult diapir presents an excellent case study of a diapir structure due to the combination of good exposure, high topographic erosional relief (i.e. < 1.5 km) and very good lateral continuity of key units flanking the diapiric core.

The post-Middle Jurassic evolution of the Central High Atlas rift basin remains less well constrained due to the scattered nature of the post-Middle Jurassic sedimentary record, which generally crops out within isolated outliers and also along the external areas of the present Atlas Mountains. New vitrinite reflectance data permit thermal modelling of the Tazoult-Amezraï area, providing key information to decipher the post-Middle Jurassic evolution of the area, currently hindered by the absence of sedimentary record.

Together, the subsidence results from the centre and periphery of the Central High Atlas Rift basin are compared to previous studies both in the same region and with other diapiric regions extending from the Atlantic margin in Morocco to Algeria and Tunisia (Fig. 1).

1. The Central High Atlas

1.1. Post-Variscan evolution of the Central High Atlas

The current structure of the Central High Atlas (CHA) in Morocco, as well as its high elevation, is interpreted as the result of the Tertiary tectonic inversion of the Mesozoic Atlas rift basin (e.g., Beauchamp et al., 1999; Frizon de Lamotte et al., 2000; Teixell et al., 2003;

Arboleya et al., 2004). The CHA Mesozoic rift basin was located in the South Tethyan passive margin and developed in the context of the opening of the Atlantic Ocean (Ellouz et al., 2003). Most authors consider the basin to be an example of multi-rift processes, with distinct rift episodes in both the Triassic and Jurassic (i.e. Fig. 3). The first rift phase (phase 1) of the Central High Atlas basin, considered to represent the eastern propagation of the central Pangea breakup, is characterised by Upper Triassic continental arid red bed deposits (Oujidi et al., 2000; Courel et al., 2003) and the local development of thick evaporitic successions. Both accumulated in fault-controlled depocentres that occur from the Atlantic Moroccan margin in the west to Algeria and Tunisia in the east (Le Roy & Piqué, 2001; Ellouz et al., 2003; Laville et al., 2004; Frizon de Lamotte et al., 2008; Gouiza et al., 2010). Exposed examples of the NE-SW trending normal fault-bound Triassic rift basins only crop out in the Marrakech High Atlas (Fig.1). Based on a detailed structural analysis of around 200 km of the Tizi n'Test fault zone, Domènech et al. (2014) determined a highly fragmented fault zone, where the faults controlling the opening of the Triassic basin were arranged as a wide deformation band. Both symmetric and asymmetric grabens would compose an extensional basin including a paleohigh that separated the Atlantic and the Tethyan domains. These grabens were bounded by high angle normal faults with a dominant dip slip movement and reveal clear thickness variations within the half graben fills that are up to 2 km thick (Baudon et al., 2009; Domènech et al., 2014). In the Late Triassic-Early Jurassic climatic setting (Courel et al., 2003; Turner & Sherif, 2007) evaporite deposition is, based on the current distribution of salt diapiric structures, thought to have occurred in the basin centre perhaps controlled by topography inherited by the rift. These evaporites were followed by a marine transgression during the Early Jurassic (Hettangian?-early Sinemurian), associated with sedimentation reflecting arid conditions (Wilmsen & Neuweiler, 2008; Lachkar et al.,

2009). It was during the Early Jurassic that the Central and Eastern High Atlas rift basin changed into marine conditions.

The second rift phase (phase 2) is thought to be the post-Hettangian reactivation of the Late Permian-Late Triassic western Tethyan rift (i.e., Frizon de Lamotte et al., 2008; Frizon de Lamotte et al., 2009). A review of the literature indicates that the precise timing of the Early Jurassic rift and post-rift phases is contestable (Fig. 3). Some authors indicate Sinemurian and Pliensbachian ages for phase 2, followed by a post-rift stage characterised by low subsidence rates linked to thermal subsidence (but may include some subsidence peaks), (i.e. Ellouz et al., 2003; Frizon de Lamotte et al., 2009; Lachkar et al., 2009). In contrast, Brede et al. (1992), Laville (2002) and Laville et al. (2004) proposed that phase 2 terminated in the earliest Jurassic and was followed by a post-rift stage during the middle and late Early Jurassic, with only local and low activity of extensional pre-existing faults (Fig. 3). According to these authors, from Toarcian to Bajocian-Bathonian (?), the region was under a transtensional regime with development of deep troughs and coeval volcanic intrusions. The differences in proposed time for the rifting stage in the Central High Atlas (from Early to Middle Jurassic) are associated with the almost lack of normal faulting cutting post-Lower Jurassic strata. Along with the lack of observed normal faulting affecting post-Lower Jurassic units, the Central High Atlas was characterised by significant salt diapiric activity, recently described by Saura et al. (2014), although it had been shown with a variable degree of detail in earlier studies (Bouchouata et al., 1995; Michard et al., 2011). According to Saura et al. (2014), the diapiric activity in the Central High Atlas covers a time range from Pliensbachian up to Callovian times and is thus partially coeval to major rifting phases during the Jurassic.

Here, in tectonostratigraphic terms we recognise three distinct domains in the Central High Atlas basin within the Jurassic rift phase (phase 2) (Fig. 2): a stable domain bounding the basin (i.e. the Saharan craton to the south; Warme, 1988; Laville, 1988); a fault block

domain, that appears to lack salt tectonics and an unstable domain with elongated ridges cored shales and evaporites that are interpreted as Jurassic aged diapiric structures (i.e. Saura et al. 2014). The latter domain has a complex palaeogeography and subsidence history reflecting the localised influence of salt diapirism.

In this overall setting, shallow water Lower Jurassic carbonate platforms nucleated both along the basin margin, and along localised tectonic/salt tectonic highs. Deeper basinal areas and troughs/minibasins experiencing higher subsidence rates were filled with deep-water limestones and marls. Major tectonic reorganisation in the Central High Atlas occurred during the late Bathonian, when carbonate platforms were progressively overlaid by deltaic and continental sediments (Ellouz et al., 2003).

During Late Jurassic and Early Cretaceous, an important magmatic activity occurred in the Central High Atlas. This was recorded by the emplacement of igneous bodies dated up to 150 Ma in the cores of ridges (now defined as diapirs by Saura et al. (2014)) and the local deposition of lava flows dated up to 110 Ma (Frizon de Lamotte et al., 2008; Charrière et al., 2011; Michard et al., 2011). During this period, continental red beds were deposited, followed by deposition of Upper Cretaceous carbonates. In contrast to the Jurassic succession, Cretaceous strata show relatively uniform thickness distribution along the High Atlas (Gouiza et al., 2010), recording a more uniform subsidence distribution during post-rift conditions (Ellouz et al., 2003). The post-rift stage lasted up to the onset of the inversion of the Atlas range that possibly started during the Late Cretaceous, although this is contested (Frizon de Lamotte et al. 2009; Frizon de Lamotte et al., 2011; Babault et al., 2013).

1.2. Djebel Bou Dahar area

The Djebel Bou Dahar (DBD hereafter) carbonate platform is located in the southern margin of the Early Jurassic rift basin, around 275 km eastward from the Tazoult area, in the called fault block domain (Fig 2). The DBD platform is flanked by two east-west trending synclines with thick successions, that represent Lower and Middle Jurassic depocenters (i.e. the Djebel Oukhasas syncline in the north and the Beni Bassia syncline in the South) (Du Dresnay, 1976). In contrast to the widespread development of salt diapirs in the Central High Atlas Basin, salt diapir activity is absent in the DBD tectonic block. Here extensional tectonics controlled platform-basin evolution during the Sinemurian to Early Bajocian (Merino-Tomé et al., 2012) (Fig. 4).

The DBD platform is a relatively narrow elongated platform that developed on a fault block, and locally sits directly on metamorphic basement. The carbonate nucleated during the Early Jurassic (Hettangian?-Early Sinemurian), when marine transgression was recorded in the CHA rift basin. The platform started as a broad, shallow-water carbonate system and evolved, from middle Sinemurian to the end of the Pliensbachian, into a high-relief isolated platform that developed around the footwall uplift of a rotating fault-block (Merino-Tomé et al., 2012). Excellent exposure, limited tectonic deformation and preservation of many aspects of the platform-to-basin morphology and stratal patterns allows for reconstruction of several continuous platform-to-basin profiles at different key stages of the evolution of the platform (e.g. Kenter & Campbell, 1991; Verwer et al., 2009, Merino-Tomé et al., 2012). The platform and coeval basinal deposits are divided into six sequences (Sequence I-VI in Fig. 4; Merino-Tomé et al., 2012) and palaeobathymetric criteria are discernible for each sequence in platform and basin locations that allow for a well-constrained understanding of subsidence profiles (Fig. 4). The platform drowned in the Toarcian, and its slopes are onlapped by Toarcian, Aalenian and lower Bajocian shales and, limestone–marl alternations and dark lime mudstones, representing deep-water pelagic and hemipelagic sediments. These accumulated

in palaeo-water depths exceeding the storm wave base and the base of the photic zone. This facies association makes for some uncertainties in understanding subsidence patterns during this time interval.

1.3. Tazoult-Amezraï area

The Tazoult salt diapir and Amezraï minibasin are located in the central part of the Central High Atlas rift basin (Figs. 1 and 2). The Amezraï minibasin is bounded to the north by the NNE-SSW trending Tazoult diapiric ridge (salt wall of 22 km in length) and to the south by the Jbel Azourki diapiric structure (Bouchouata, 1994; Bouchouata et al., 1995; Saura et al., 2014). In this study area it is possible to differentiate between Jurassic diapiric deformation and later Alpine deformation, due to the presence of Middle Jurassic age units, which fossilize movement on diapirs in the area (Fig.5). In addition to the structural analysis of Saura et al. (2014), understanding of the diapiric movement is constrained by the detailed sedimentological studies (i.e. Grélaud et al., 2014, Joussiaume et al., 2014). The extensive and well-preserved halokinetic strata on the flanks of the Tazoult diapir document the timing of diapir activity, that ranges from Pliensbachian to Bajocian, lasting at least 15-20 My.

Detailed 3D structural reconstruction work indicates that both the Tazoult and the Jbel Azourki diapiric structures are controlled at depth by normal faults. These constrain the extent of the Amezraï minibasin, and although there is no direct evidence of these faults at the surface, the Azourki welds are notably segmented along strike and closely mimic patterns associated with the segmented normal faults (Saura et al., 2014) (Fig. 5). This minibasin is filled with shallow marine deposits that range from Pliensbachian to Bajocian age. The lowermost part of the sedimentary succession comprises Pliensbachian shallow marine platform carbonates (Jbel Choucht and Aganane formations), overlain by the mixed siliciclastic-carbonate deposits of the Zaouiat Ahançal Group (from base to top: Amezraï,

Tafraout and Aguerd-n'Tazoult formations) (Jossen & Couvreur, 1990; Bouchouata, 1994; Bouchouata et al., 1995; Joussiaume et al., 2014). In turn, the Zaouiat Ahançal Group is overlapped by Aalenian to Bajocian shallow marine limestones of the Bin el Ouidane Group (Fig. 5). These deposits are relatively layer-cake, and appear to fossilize diapiric activity on the Tazoult ridge and subsidence of the adjacent minibasin (i.e. Saura et al, 2014, their Fig. 5).

2. Method and data

2.1. Subsidence analysis

Subsidence analysis has been performed using GENEX® 4.0.3 software in two sections of the Djebel Bou Dahar platform (Fig. 4) and in two sections of the Tazoult-Amezraï area (Fig. 5). The software calculates total and tectonic subsidence through time, based on backstripping analysis (Steckler & Watts, 1978). The subsidence analysis is performed using formation ages, formation thicknesses, lithology percentages, sedimentary environments and palaeobathymetry estimations, together with porosity/depth curves that are established by the software. GENEX® does not apply corrections that consider eustatic variations, thus the results should be interpreted while taking this assumption into account.

Platform top and basin data have been used to determine subsidence histories in Djebel Bou Dahar locality (see location in Fig. 4). In the Djebel Bou Dahar platform section, an erosional event has been defined between 195.3 and 187.3 Ma (Table 1). The amount of erosion is the difference between the present-day thicknesses of sequences I and II in the basin and platform sections, assuming that they were deposited as constant thickness units from basin to platform (see details of platform evolution in Merino-Tomé, 2012). The palaeobathymetry estimation for sequences III to VI is based on facies analysis integrated with restored platform and slope geometries, although decompaction was not considered (Fig.

4 and Table 1). Less constrained palaeobathymetric estimations correspond to the Toarcian and Aalenian, when the platform was drowned in response to the Toarcian OAE event. Condensed pelagic deposits and hard grounds typify the platform top sedimentation during Toarcian and Early Aalenian times, while pelagic sedimentation occurred in the nearby basinal areas, indicating that water depths exceeded the depths of the lower boundary of the photic zone and the base of storm waves. In the absence of good palaeontological or sedimentological criteria, the values of 100 m water depth for the platform top, and 715 m for the nearby basin section have to be considered as minimum values during the Toarcian and Aalenian periods.

In the Tazoult-Amezraï area, all of the exposed formations were deposited in shallow marine environments (here, considered within palaeo-water depths from 0 to 30 m) (Table 2). It should be noted that the values of palaeobathymetry from shallow marine depositional environments show an error which is much smaller than the values set in deep water environments (Dupré et al., 2007; Lachkar et al., 2009; Xie & Heller, 2009), thus the errors linked to palaeobathymetry estimation can be considered as minimal.

The less constrained input from the Tazoult-Amezraï case study is the thickness of lower Jurassic sedimentary units in the central part of the Amezraï minibasin. The section through the studied area (Fig. 5) displays a conservative thickness of the lower Jurassic sedimentary units and, therefore, an underestimate of thickness is expected in the central part of the Amezraï minibasin (Amezraï section, Table 2). This source of error should be considered in the resulting subsidence evaluation. Additionally, no Hettangian-Sinemurian strata are exposed in the area (but they do occur as inclusions within the diapirs), although the Sinemurian Bou Imoura Fm. is exposed 20 km to the north, where it reaches a thickness of c.1000 m (Grélaud et al., 2014). Given the above considerations, the subsidence history in this case study can only be accurately shown from the beginning of the Pliensbachian.

Erosional events have not been identified in the Tazoult-Amezraï area, however, in the Tazoult ridge section a non-depositional event is defined between 175 and 171.1 Ma (Hiatus in Table 2) whereas the sedimentary record is continuous from the Early to the Middle Jurassic in the Amezraï section (Table 2).

2.2. Thermal model

The thermal models presented in this study have been calculated with GENEX® software using data from Tazoult-Amezraï area (Amezraï section, Table 2). The input data for this modelling are: geological events such as deposition of the sedimentary units (including ages, thicknesses and lithological composition) and erosional events (including ages and amount of eroded deposits), petrophysical properties of the sedimentary units (in the present study we used the default properties established by the software), and thermal parameters (paleo heat flow). The output of this modelling is the thermal history of each sedimentary unit and of the entire sedimentary record. Consequently, we obtain the evolution of temperature and evolution of the maturity of organic matter in the studied basin.

From field outcrops and structural and sedimentological studies, we have defined the geological events from Pliensbachian to Bajocian in the Amezraï section (Table 2), which do not include any quantified erosional event. In contrast, in our modelling process the surface heat flow prior to the onset of sedimentation (paleo-heat flow) and potentially post-Bajocian eroded deposits are undetermined parameters. The calibration of these parameters is based on the comparison between reflectance vitrinite data obtained from samples collected in the Tazoult-Amezraï area and the theoretical reflectance vitrinite curves calculated by the software. In this case, GENEX® calculated two different vitrinite reflectance curves: Easy%Ro curve, based on Sweeney and Burnham (1990) and Sweeney et al. (1990), and IFPRo reflectance curve, that is constructed using a global database.

Twenty-seven vitrinite samples have been collected throughout the Tazoult-Amezraï area (Figs. 5 and 6), with the most continuous sampling along the Aguerd-n'Tazoult Formation, the uppermost part of the mixed siliciclastic-carbonate succession. Generally, the vitrinite reflectance values range from 0.81 to 1.98%. Nevertheless, some of the samples show anomalously high values of vitrinite reflectance reaching a reflectance of 3.05% (e.g., ES 797). These samples were collected not far to those diapiric structures (i.e. < 200 m) that are intruded by Middle-Late Jurassic igneous bodies and their emplacement has had a significant thermal imprint on the obtained vitrinite reflectance values (Fig. 6).

From the entire vitrinite dataset, we selected samples that are located closest to the case study stratigraphic section as constraints on the thermal modelling. The presence of diapir structures produces thermal anomalies due to the high thermal conductivity of the salt (Petersen & Lerche, 1996; Magri et al., 2008). Because of the potential impact of diapirs in the thermal field, we only use the Amezraï minibasin section and associated vitrinite samples to carry out the thermal modelling. The thermal model is constrained by 14 samples (black samples in Fig. 6), with a reflectance mean value of 1.53%, with absolute values that progressively decrease towards the top of the succession (i.e. to 1.21%), showing a good fit with their relative stratigraphic position (Fig. 6).

3. Early-Middle Jurassic 1D subsidence curves

3.1. Subsidence evolution of the Djebel Bou Dahar carbonate platform

As introduced earlier, the well-preserved carbonate platform-top to basin profiles of the Djebel Bou Dahar platform (Fig. 4) reveal stratal geometries, that have undergone relatively little deformation and allow reconstruction of primary carbonate platform-basin relief (platform slope height from basin floor areas) throughout its evolution (Verwer et al., 2009; Merino-Tomé et al., 2012). Subsidence analyses have been performed in two locations:

platform top and basin. The platform top subsidence curve (Fig. 7a) shows two short episodes of subsidence (Early Sinemurian and Late Pliensbachian, respectively), separated by a period of mild uplift during the time in which normal faults were active (Late Sinemurian – Early Pliensbachian). This was followed by a period of quiescence around the end of the Toarcian-Bajocian (i.e. Middle Jurassic). The first subsidence event occurred during Early Sinemurian (deposition of sequences I and II) with a tectonic subsidence rate of 0.03 mm yr^{-1} and the rate of total subsidence is around 0.05 mm yr^{-1}. The second step of subsidence occurred at rates up to 0.04 mm yr^{-1} during the Late Pliensbachian (deposition of sequences V and VI). The total subsidence rates are also low, but slightly higher than tectonic subsidence rates, reaching values up to 0.05 mm yr^{-1} (Fig. 7a).

The subsidence curve of the basin area shows a unique subsiding event spanning between the Sinemurian and Pliensbachian periods (~17 Myr), followed by a stage of almost no subsidence during the Toarcian and Aalenian periods (~12 Myr) (Fig. 7). The Sinemurian-Pliensbachian period shows tectonic subsidence rates of 0.03 mm yr^{-1} and the total subsidence is around 0.05 mm yr^{-1}, increasing slightly up to 0.06-0.08 mm yr^{-1} for both tectonic and total subsidence from the Early-Late Sinemurian boundary onwards (Sequence III base), coinciding with the onset of the southwards tectonic rotation of the DBD block and renewed extensional fault activity. The close parallel evolution of both tectonic and total subsidence curves indicates that most of this subsidence is tectonic, as proved by the syndepositional activity of the normal faults bounding the basin (Merino-Tomé et al., 2012) (Fig. 7).

In the platform domain, the subsidence model includes the thickness of sequences I and II (Lower Sinemurian), equivalent to those measured in the basin. During the sedimentation of these two units during early Sinemurian times, the first step of subsidence

occurred at rates of 0.05 mm yr^{-1}, which showed a uniform distribution across the entire DBD platform. A major erosion surface is present between sequences II and V (Late Sinemurian-Early Pliensbachian), related to the uplift of the footwall of the DBD fault block and southward tilt due to the activity of the N-dipping bounding normal fault (Merino-Tomé et al., 2012). As a result of this local erosion, the subsidence curve corresponding to the platform top shows a limited uplift from Late Sinemurian to Early Pliensbachian. This uplift is coeval to the increase in subsidence rates in the basin area. During Toarcian and Aalenian, a ceasing of the subsidence is recorded in the entire area.

3.2. Subsidence evolution in the Tazoult ridge and Amezraï basin; High Atlas diapiric province.

The previous section examined the timing and rates of subsidence from the flanks of the High Atlas basin during the Early Jurassic. This allows us to establish base line subsidence rates and the timing of rift and post rift subsidence phases for phase 2 rifting in the absence of diapiric processes. This section aims to establish the subsidence of the southern flank of the Tazoult ridge and the centre of the adjacent Amezraï basin that are impacted by diapiric processes.

The Tazoult ridge and the Amezraï basin subsidence curves both show a similar trend, but they are different in terms of the rates and amounts of total subsidence (Fig. 8). Both sections show a significant subsidence event from the Sinemurian-Pliensbachian boundary at ~190 Ma to the end of the Aalenian at ~170 Ma, with two rapid periods of subsidence separated by a period of lower subsidence rates during Late Pliensbachian and Toarcian times (Fig. 8).

The first tectonic subsidence event that can be constrained in the Tazoult diapir flank occurred in the Early Pliensbachian (deposition of Jbel Choucht and Aganane formations) at

rates of 0.15 mm yr^{-1}. From Late Pliensbachian to Toarcian, the subsidence rate decreased to 0.01 mm yr^{-1}, reaching a period of quiescence, lasting for about 4 Myr in the Toarcian-Aalenian transition. This quiet period encompassed the deposition of Tafraout and lowermost Aguerd-n'Tazoult formations in the central part of the basin. The final period of rapid tectonic subsidence occurred from the Aalenian to Bajocian periods, attained rates of 0.27 mm yr^{-1}, and was synchronous with deposition of the upper Aguerd-n'Tazoult and Bin el Ouidane 1 formations (Figs. 5 and 8). The total subsidence rates of the same periods are 0.22, 0.09 and 0.74 mm yr^{-1} respectively.

In the Amezraï basin, the first constrained Early Pliensbachian tectonic subsidence event occurred at rates of 0.17 mm yr^{-1} (Fig. 8). These rates are similar to those reported for the Tazoult diapir (Fig. 8). The following two periods, show comparable trend with the Tazoult section, but with higher tectonic subsidence rates of 0.06 mm yr^{-1} and 0.32 mm yr^{-1}, respectively during the late Pliensbachian-Toarcian and Aalenian. Total subsidence rates display the same trend, changing from 0.38 to 0.19 and finally to 0.98 mm yr^{-1}.

Major differences between Tazoult and Amezraï subsidence curves occurred during Late Pliensbachian times, when the rapid deposition of the mixed carbonate-clastic Amezraï Formation occurred in the basin centre. It was the deposition of this unit that appears to have triggered the development of allochthonous salt sheets in both Tazoult and Jbel Azourki salt walls (Fig. 4) (Saura et al., 2014).

4. Tazoult-Amezraï thermal modelling

To ascertain the post-Middle Jurassic geological history of the study region is not straightforward due to the general scarcity of sedimentary record in the Central High Atlas. However, scattered synclines from the external parts of the Atlas (Ouaouizaght, Iouaridène and Aghzif-Nadour synclines) show concordant thin and probably condensed Upper Jurassic-

Lower Cretaceous red beds successions with thickness up to 1800 m (Ellouz et al., 2003; Haddoumi et al., 2010). Apatite fission track dating along the Imilchil transect indicates more than 1.5 km of sedimentary burial after the emplacement of the Middle-Late Jurassic volcanic intrusions (Barbero et al., 2007) (Fig. 9).

Contrarily, the Anoual and Aït Attab synclines show a sedimentary succession punctuated with unconformities or periods of potential non-deposition (sedimentary hiatus), which are diachronous through synclines (Haddoumi et al., 1998; Haddoumi et al., 2008). Oxfordian to Kimmeridgian and Valanginian to Barremian in the Anoual syncline and Bajocian and Barremian in the Aït Attab.

In our work we use these data to constrain ages of post-Middle Jurassic deposition to build two models: one with concordant sedimentation and one involving potential large-scale vertical uplift events occurring during the Late Jurassic and Lower Cretaceous periods as suggested by authors working in this region.

This second model involving vertical motions of the West Moroccan Arch and extending eastward within the Central High Atlas during Upper Jurassic and Lower Cretaceous times has been postulated by Frizon de Lamotte et al. (2009). This large-scale thermal doming has been recorded using thermochronology on Palaeozoic samples from the surrounding Moroccan Meseta and the Anti Atlas (Ghorbal et al., 2008; Missenard et al., 2008; Balestrieri et al., 2009; Saddiqi et al., 2009; Ruiz et al., 2011; Domènech, 2015) (Fig. 9). Local sedimentary hiatus, like the ones described in the syncline bordering the Central High Atlas, are used by these authors to reinforce Late Jurassic-Early Cretaceous widespread uplift interpretation

In the next sections we constrict the undetermined parameters (paleo-heat flow and additional sedimentation) for the two contrasting proposed scenarios for the post-Middle Jurassic evolution of the Central High Atlas. 1) Thermal models with sedimentation during

Upper Jurassic and Lower Cretaceous times and 2) Thermal models considering Late Jurassic-Early Cretaceous exhumation in the Central High Atlas. These scenarios provide two end-members for the unconstrained part of the evolution of the Tazoult-Amezraï area.

4.1. Thermal models with sedimentation during Early Jurassic and Late Cretaceous times

Numerous thermal models have been made to test different possibilities for both heat flow estimations during rift and post-rift periods. Post-rift heat flow has been set at 60 mW/m^2 in agreement with thermal models and present-day heat flow regional data in the Central High Atlas (Rimi et al., 2005; Zeyen et al., 2005). Heat flow during rifting (paleo-heat flow), as well the total duration of it, however, is more complex to define and we can only put certain limits to try to constrain the observed data. For this reason, we show the following 6 models (Fig. 10): a) short rifting event (189 to 182.7 Ma) and low paleo heat flow (70 mW/m^2) based on the thermal models of Sachse et al. (2012) in the Middle Atlas; b) short rifting event (189 to 182.7 Ma) and higher paleo heat flow (105 mW/m^2) according to the higher value compiled in rifted basins (Allen and Allen, 2005), as well as to the mean value of heat flow calculated in the eastern arm of the East African Rift System, dominated by volcanics (Morgan 1983); c) short rifting event (189 to 182.7 Ma) and very high paleo heat flow (120 mW/m^2) based on the highest value in basins with deep lithosphere involvement (Allen and Allen, 2005); d) e) and f) long rifting event (189 to 140 Ma) and paleo heat flows of 70, 105 and 120 mW/m^2, respectively. All models include Alpine inversion of the Central High Atlas divided in two steps, from 80 to 35 Ma (35% uplift and erosion) and from 35 to 0 Ma (65% of uplift and erosion), based on published works about Central High Atlas inversion (Fraissinet et al., 1988; Görler et al., 1988; Teixell et al., 2005; Tesón & Teixell, 2008; Tesón et al., 2010).

The models using paleo heat flow values of 70 mW/m^2 are considered to be a minimum result with maximum additional sedimentation (burial), whereas, the very high value of 120 mW/m^2 is considered as maxima with minimum burial. The long period of rifting includes rifting and post-rift period, which is characterised by continuous intrusions of volcanic and subvolcanic rocks within the Central High Atlas crustal levels and thus potentially increasing the paleo heat flow up to the early Lower Cretaceous at about 140 Ma (e.g., Frizon de Lamotte et al., 2008; Charrière et al., 2011; Michard et al., 2011). One important result is that all models required additional sedimentary burial to fit the reflectance of vitrinite curve (Fig. 10). This additional burial would consist of post-Bajocian sediments completely eroded during the Alpine compression (from 80 Ma to present-day).

The models with the lower rifting paleo heat flow values (models a and d) need additional sedimentary burial ranging from 2400 to 2200 m. Intermediate paleo-heat flow models (b and e) need 2000 to 1200 m of extra burial whereas high paleo-heat flow models (c and f) still need between 1700 and 800 m of post-Bajocian extra burial. Although all presented models are geologically possible, we use in our work the intermediate paleo-heat flow models with 105 mW/m^2, corresponding to the maximum value documented in rift basins (Allen and Allen, 2005), to get the minimum amount of post-Bajocian extra burial and a geohistory (burial history plot) with minimum values of subsidence during rift and post-rift periods for both scenarios with sedimentation and with uplift and erosion during the Late Jurassic and Early Cretaceous periods.

4.2. Thermal models considering Late Jurassic-Early Cretaceous exhumation in the Central High Atlas basin

Numerous pointers suggest Late Jurassic-Early Cretaceous uplift in NW Morocco, mostly along the Western Moroccan Arch (parallel to the Jurassic Atlantic Moroccan margin) and Anti-Atlas domain (parallel to the southern border of the Jurassic Atlas rift basin), based on thermochronological studies (Ghorbal et al., 2008; Saddiqi et al., 2009; Ruiz et al., 2011; Domènech, 2015) (Fig. 9). The inferred spread of such uplift inside the Jurassic Atlas rift basin has been associated with the massive post-rift magmatic event (see the review in Frizon de Lamotte et al., 2015). The ending of this thermally-related uplift could range from 140 to 110 Ma (Frizon de Lamotte et al., 2008). Nonetheless, no direct indications are available in the central part of the Central High Atlas, where younger preserved sediments are Callovian in age (~163.5 Ma).

In order to check the effects of this presumed Late Jurassic exhumation in the geohistory of the Tazoult-Amezraï study region, we ran a new set of models, assuming a few undetermined parameters to fit results with the reflectance of vitrinite data: a) long duration (189-140 Ma) and elevated heat flow (105 mW/m^2) followed by heat flow of 60 mW/m^2; b) 170 to 163.5 Ma sedimentation with average rates equal to previous Early-Middle Jurassic rates (0.22 $mm.yr^{-1}$) amounting to 1430 m; c) inferred uplift from 163.5 to a maximum younger age of 129.4 Ma (first dated Cretaceous deposition preserved in most external Atlas basin domains, although some of the synclines contain older deposits with an age between Middle Jurassic to Barremian), that would imply an erosion equivalent to a previously deposited 1.43 km of Middle-early Late Jurassic deposition in the centre of the Central High Atlas basin; d) deposition of an unknown thickness of Cretaceous sediments to be determined during the modelling; e) Alpine inversion of the Central High Atlas in two steps from 80 to 35 Ma (35% of uplift) and from 35 to 0 Ma (65% of uplift).

The model results indicate that about 1600 m of Cretaceous burial is needed to fit the reflectance of vitrinite data for chosen parameters (Fig. 11a). Extending the 105 mW/m^2 to 110 Ma would reduce the Cretaceous amount of burial to 1200 m (Fig. 11b). Yet, the geohistory for this second scenario, characterized by Late Jurassic and Early Cretaceous uplift, shows a more intricate history and is not easy to associate it with geological observations within the study area, but is also shown in the geohistory plots (Fig. 12).

4.3. Central High Atlas geohistory

Results of the subsidence analysis of the Amezraï basin have been coupled to the results from thermal modelling in order to build a complete geohistory for this part of the Central High Atlas (Fig 12). From all the thermal models that have been presented above, we selected the model with a long high thermal event of 105 mW/m^2 (Fig. 10e) and 1200 m of additional deposition at a roughly continuous sedimentation from the Upper Jurassic to the onset of the Alpine inversion (80 Ma), as was proposed in the subsidence models of Ellouz et al. (2003) for several locations in the Central High Atlas.

As shown in Fig. 12, the Amezraï basin shows that the peak of organic matter maturity was reached during the Late Cretaceous. The Lower Jurassic deposits (Jbel Choucht-Aganane and Amezraï formations) would have entered into the gas window during Middle Jurassic times, and then became over mature during Upper Jurassic and Lower Cretaceous times. In contrast, the Middle Jurassic sediments (Tafraout, Aguerd-n'Tazoult and Bin el Ouidane 1 formations) came into the oil window (vitrinite reflectance between 0.7 and 1.3%) early after their deposition and remained between the oil and gas windows up to the end of the continuous subsidence period (Upper Jurassic to Lower Cretaceous), preceding the basin inversion and exhumation starting in the latest Cretaceous.

Figure 12 also shows the evolution of the base of the analysed sedimentary succession (base of Jbel Choucht Fm., grey line) for the second tectonic scenario, characterized by Late Jurassic-Early Cretaceous uplift of the western domain of the Central High Atlas as previously discussed.

5. Discussion

5.1. Rifting subsidence evolution of the Central High Atlas

The Central High Atlas underwent Triassic rifting (phase 1) and Lower Jurassic rifting (phase 2) as shown in Fig. 3. The lack or non-observation of Triassic rift deposits in both the study area and the Middle Atlas does not permit to model this first rift phase (Fig. 13). Thus, this Triassic rift phase 1 is only indicated in the Aït Chedri Tizgui onshore locality in the Atlantic Moroccan Atlas (ACT in Figs. 1 and 13). This locality subsided ~3.4 km during the Triassic, as also evidenced in its continuation in the Agadir Basin (Zühlke et al., 2004) and in the offshore seismic lines (Hafid et al., 2008; Tari & Jabour, 2013). The Aït Chedri Tizgui in the Atlantic Atlas shows a rather continuous sedimentation from the Jurassic to present day, consistent with a passive margin setting (ACT in Fig. 13). The Triassic rift phase 1 is also recorded in well-developed half graben structures with thick siliciclastic sedimentary successions in several localities of the Western High Atlas (e.g., Baudon et al., 2009; Redfern et al., 2010; Domènech et al., 2014).

Conversely, the subsidence curves for the Lower Jurassic rift phase (phase 2) can be calculated all around the Central High Atlas and the Middle Atlas. During rift phase 2, the Lower Jurassic basin geometry comprised a number of NE-SW oriented tectonic highs separating deeper basins (Fig. 2). The compartmentalization between tectonic highs and basins is mostly indicated by changes in sedimentary facies and thicknesses owing to the

scarcity of normal faults cutting Jurassic sediments. This is due to the existence of Upper Triassic evaporitic mobile rocks that constitute a decoupling layer between basement faults and Jurassic stratigraphy at depth. Subsidence histories were complex, depending on this paleogeography and thus published subsidence analyses may show local rather than rift basin scale results (e.g. Poisson et al., 1998; Bracène et al., 2003; Ellouz et al., 2003; Patriat et al., 2003; Lachkar et al., 2009). Therefore, the comparison of subsidence curves from the Central High Atlas with other curves from the Central High Atlas can help to better understand the tectonic framework of the rift basin in which the Djebel Bou Dahar and the Tazoult-Amezraï localities are placed.

We first compare our results with subsidence curves derived from the margins of the Central High Atlas rift basin (High Plateau and Missour Basin; Ellouz et al., 2003) (HP and MB, respectively in Figs. 1 and 13). These curves are relatively smooth and show low subsidence rates (< 0.02 $mmyr^{-1}$) during the Jurassic and through the Cretaceous and Palaeogene periods, exemplifying the stable domain of the rift basin (Fig. 2). In contrast, subsidence curves from the centre of the rift basin tend to show a short period of rapid subsidence during the Lower Jurassic (Sinemurian-Pliensbachian), followed by slower subsidence rates that may continue until the uppermost Middle Jurassic in the High Atlas locality comprising the Foum Zabel (Lachkar et al., 2009), the High Atlas Border (Ellouz et al., 2003), the Djebel Bou Dahar basin and the Amezraï basin curves (FZ, HAB, Djebel Bou Dahar and Amezraï in Fig. 13).

The comparison between Djebel Bou Dahar subsidence curves with those presented in the Rich region about 100 km to the west of the study area by Lachkar et al. (2009) and Quiquerez et al. (2013), is important to better constrain the Early Jurassic rift phase along the Fault Domain on the southern border of the Central High Atlas basin (see location in Figs. 1 and 2). Lackhar et al. (2009) presented three different tectonic subsidence curves from the

Rich transect where carbonate platforms developed on top of an extensional system. These subsidence curves correspond to three faulted blocks showing differential subsidence evolution from the margin to the inner part of the basin (Fig. 14). The Djebel Bou Dahar platform top subsidence curve is comparable to the Boutazart curve (Fig. 14). This latter curve corresponds to the shallower part of the rift basin in the Rich transect. Both, the Djebel Bou Dahar and Boutazart subsidence curves, show a similar evolution corresponding to platform settings (Fig. 14). During the Late Sinemurian and Pliensbachian periods, the Boutazart section records a tectonic quiescence period with tectonic subsidence rates lower than 0.008 mmyr-1 (Lachkar et al., 2009), whereas in the DBD platform, the top curve shows a period of mild uplift followed by a renewed subsidence stage (0.04 $mmyr^{-1}$). The differences between both localities are interpreted as a result of a different range of normal fault activity, being more intense in the DBD area.

Subsidence curves obtained using data from more basinal settings in the Rich transect (Foum Zabel and Guerss curves in Fig. 14) also show trends that are different to the Djebel Bou Dahar basin curve. The Foum Zabel section shows a period of low tectonic subsidence (0.01-0.03 mmyr-1) during the Early Sinemurian, followed by a very high subsiding episode (average rate of 0.50 mmyr-1) from late Sinemurian to the end of Pliensbachian times. The Guerss section (central part of the basin) shows a maximum tectonic subsidence during the Early Sinemurian, with tectonic subsidence rates ranging from 0.17 to 0.77 mmyr-1 (Lachkar et al., 2009). Both sections differ from the continuous subsiding curve (0.06 mmyr-1) of the Djebel Bou Dahar basin section, in terms of rates and timing of maximum subsidence. The substantial larger tectonic subsidence rates for the deep marine basins in the Rich transect, compared to the well-constrained Djebel Bou Dahar transect is the consequence of applying significantly larger paleobathymetric estimations in the former locality (Dupré et al., 2007; Lachkar et al., 2009; Xie & Heller, 2009).

All analysed subsidence curves, nonetheless, indicate a rifting episode from Sinemurian to Pliensbachian times with a diachronous fault activity, as pointed out by the subsidence variations through time. This Sinemurian to Pliensbachian time range, shorter than the rifting phase reported in the Middle Atlas by Zizi (1996), is in agreement with observed tectonostratigraphic relationships reported by Poisson et al. (1998) from Tinjdad area (see location in Fig. 1) where Toarcian marls fossilised pre-Toarcian normal faults. Generally, the tectonic subsidence rates recorded in the faulted domain are lower in the shallower areas of DBD and Rich transect (< 0.1 $mmyr^{-1}$), whereas the tectonic subsidence rates reached high values in the basinal domain (up to 0.7 $mmyr^{-1}$). High subsidence rates were also recorded in the HAB curve described by Ellouz et al. (2003), which corresponds to the northern border of the Central High Atlas basin (Fig. 13).

The Amezraï basin subsidence curve is nevertheless the most distinctive in the Central High Atlas basin showing very rapid overall subsidence rates up to 0.98 $mmyr^{-1}$ during Early to lowermost Middle Jurassic times, even when using low values of paleobathymetry (Figs. 8 and 13). Given the well-documented diapiric structures in this area, we interpret that this fast subsidence event was related to a combination of both normal faulting and diapiric salt withdrawal from the basin centre, coeval with salt extrusion along the salt walls that characterised the Tazoult and Jbel Azourki ridges (e.g., Saura et al., 2014) (Fig. 5). Here, there is a good match in time between the onset of the second period of rapid subsidence in the Amezraï minibasin (i.e. Late Pliensbachian-Aalenian) and the initiation of inflation of the Tazoult and Azourki allochthonous salt bodies adjacent to the Amezraï minibasin (Fig. 13).

Quantification of fault activity and salt withdrawal during the Lower Jurassic subsidence phase is not straightforward due to the lack of outcrops with which to estimate the thickness variation of the ductile evaporite-bearing unit. However, the high tectonic and total subsidence rates (0.32 and 0.98 $mmyr^{-1}$, respectively) (Fig. 13), compared to purely

extensional tectonics recorded in the Djebel Bou Dahar or other areas of the basin margin, strongly suggest a salt tectonics contribution, as has been reported in other salt basins worldwide (Wilson et al., 1989; Hodgson et al., 1992; Dupré et al., 2007; Hudec et al., 2009). In this scenario, the active interaction between sedimentation and salt movement could lead to cyclic acceleration of local sedimentation rates, salt withdrawal and creation of accommodation, resulting in the observed increase in the subsidence rate.

5.2. Post-rift evolution of the Central High Atlas

The post-Middle Jurassic evolution of the Central High Atlas rift basin remains less well constrained, due to the scattered nature of its younger sedimentary record, which generally crops out within isolated outliers and also along the marginal areas of the present Atlas Mountains. The thermal and burial models for the Tazoult-Amezraï basin transect, allow us to infer some key elements of the post-Middle Jurassic evolution of this area. We discuss two potential geohistory models for the Central High Atlas rift basin (Tazoult ridge and Amezraï minibasin) in which results are directly constrained by our thermal study based on reflectance of vitrinite data: our preferred model, characterised by a roughly continuous but small sedimentary record from Late Jurassic to Late Cretaceous and an alternative model characterized by Late Jurassic-Early Cretaceous uplift event.

The results from our first set of models show that whatever is the amount of heat flow applied and its duration the Tazoult-Amezraï area needed an extra burial ranging from 800 to 2400 m. Considering the model from Fig. 10e with a heat flow of 105 mW/m^2 from 189 to 140 Ma (selected for geohistory plots), the additional sedimentary burial is of 1200 m.

Other localities around the Central High Atlas show burial histories that are directly comparable to the results presented here. Ellouz et al. (2003) reported c. 1800 m of post-Bajocian deposits in the northern border of the Central High Atlas. Apatite fission track data

(Barbero et al., 2007) also indicate a significant overburden of more than 1500 m in the Imilchil transect to the east of the study area, as well as a continuous exhumation starting in the latest Cretaceous. Haddoumi et al. (2002) and Haddoumi et al. (2010) also described several hundred metres of Upper Jurassic to early Upper Cretaceous aged "couches rouges" (i.e. red beds) cropping out in the Ouaouizaght syncline (located near HAB in Fig. 1). These sedimentary sequences display growth patterns with ages ranging from late Bathonian to late Barremian and thus pointing to a probable diapiric evolution persisting from Late Jurassic to middle Early Cretaceous (~167 to 127 Ma). Using illite "crystallinity" analysis, Brechbühler et al. (1988) determined a 6 km thick sedimentary pile of post-Toarcian sediments in the Errachidia-Midelt transect, located 162 km eastward of the Tazoult-Amezraï area. In summary, post-Middle Jurassic burial seems generalised in the Central High Atlas sedimentary basin.

The alternative scenario proposing the western segment of the Tethyan Atlas as uplifted after Middle Jurassic times (e.g., Beauchamp et al., 1999; Frizon de Lamotte et al., 2008) has also been tested by means of thermal modelling and the results included in the geohistory plots (Figs 11 and 12). This model, however, has been constructed assuming two consecutive poorly constrained subsidence-uplift events from the Late Jurassic to present day. In our study, the fit of this scenario with the thermal modelling has been obtained by applying around 1.43 km of deposition followed by the same amount of erosion during the Late Jurassic-Early Cretaceous event and around 1.6 km (same amount of sedimentation and erosion) during the Alpine event. Hence, although presented results provide a suitable fit with the reflectance of vitrinite thermal data, the complexity of the geological processes involved in such a model as well as the lack of match with the geological observations in the Central High Atlas basin strongly suggest that the widening of the uplift and exhumation along the West Moroccan Arch was not reaching the study area.

5.3. Along-strike subsidence variations of the Atlas from Morocco to Tunisia

The Atlas system can be divided into two major domains: the Atlantic and the Tethyan provinces having different subsidence histories (Le Roy et al., 1998; Le Roy & Piqué, 2001; Frizon de Lamotte et al., 2008; Frizon de Lamotte et al., 2011) (Fig. 15). The Atlantic domain, corresponding to the Western Atlas and offshore Morocco, is characterised by a major Triassic rifting stage inferred to have evolved into a drift stage from the Early Jurassic to the Late Cretaceous (Hafid, 2000; Zühlke et al., 2004; Hafid et al., 2008) (Aït Chedi Tizgui; ACT in Fig. 15). In the Central Atlas (Tethyan domain), a distinct second rift phase occurred during Lower Jurassic times (Figs. 3, 13, 14 and 15).

The analysis of the variations of the subsidence history along the axis of the Atlas rift system in the Tethyan domain is not intended to be conclusive and only aims to give some thoughts about these variations from Morocco to Tunisia, based on available subsidence studies when integrated with our studies. It is important to realise during this evaluation that subsidence curves are strongly influenced depending on used data, methodology and on their tectonic locations, so that direct comparisons are not always forthright. Despite these potential complications, we contrast three different subsidence analyses along the strike of the Atlas basin: the total and tectonic subsidence curves for the Amezraï basin in the west (Central High Atlas in Morocco; CHA), the total subsidence curve from the Bled Chetihat basin in the Saharan Atlas in Algeria (SA in Fig. 15), and the tectonic subsidence curve of the Gabés Basin in the Tunisian Atlas (Bracène et al., 2003; Patriat et al., 2003) (GB in Fig. 15).

The subsidence history of the Bled Chetihat basin in the Saharan Atlas comprises the complete Jurassic, Cretaceous and Palaeogene successions (Bracène et al., 2003). The total subsidence curve shows a regional period of fast subsidence, in different steps, from Lower Jurassic to middle Cretaceous times, followed by a period of slow subsidence in order to reach the upper part of the Oligocene. During late Oligocene this time, the top of the Upper Triassic unit reached its maximum depth at > 6 km below sea level, just before the onset of

exhumation (Fig. 15). The Triassic top is located at depths of 4.2 km, at present elevated during the Atlas tectonic inversion (Bracène et al., 2003; their Fig. 13). Interpreted seismic lines in the western Saharan Atlas show the deepest synclines that are still located at depths of ~6 km (Bracène et al., 2003; their Fig. 16).

Subsidence analysis shows low subsidence rates of 0.05 mm yr-1 in Early and Middle Jurassic times, followed by a period of larger subsidence (up to 0.20 mm yr-1) during Late Jurassic and Early Cretaceous times. This second period of fast subsidence is synchronous to diapiric growth and salt withdrawal from basins, which probably increased subsidence rates (Fig. 15). Afterwards, the subsidence curve shows a slow period of subsidence up to the late Oligocene prior to widespread uplift during the Neogene and the main inversion in the late Lutetian (discussed but not shown in the SA subsidence curve of Bracène et al., 2003) (Fig. 15).The subsidence histories of Chotts, Gabès and Hammamet basins in southern Tunisia have been analysed by Patriat et al. (2003) (see their Fig. 11). These authors divide the subsidence history into three main events, evolving from rifting to compression, as displayed in the tectonic subsidence curve for the Gabés Basin (GB in Fig. 15). The Lower Jurassic to Aptian-Albian boundary main rifting period is characterised by a long and constant subsidence with low rates of about 0.02 mm yr^{-1}. Furthermore, the Aptian to Late Cretaceous transition period is characterised by variable subsidence among different basins that is attributed to the important role of active halokinesis, working since Aptian times (Perthuisot, 1981; Snoke et al., 1988) or even older (Boukadi & Bedir, 1996). Starting in the Paleocene, inversion tectonics affected specific structures in southern Tunisia, as clearly imaged in seismic lines showing a major Oligocene post-folding unconformity. Patriat et al. (2003) concluded that salt diapirism rejuvenation and reactivation were also common during this phase of shortening, spanning from the Eocene to present day (Fig. 15).

The comparison among selected subsidence curves from the Tethys domain shows diachronous highest rates of subsidence as well as maximum burial, becoming younger towards the east (Fig. 15). In the Central High Atlas (Amezraï basin), the highest rates of tectonic and total subsidence occurred during the Early and Middle Jurassic. The maximum burial, according to the presented geohistory model, was achieved during the Late Cretaceous with maximum thicknesses of almost 5.5 km. In the Saharan Atlas in Algeria (Bled Chetihat basin), the fastest and maximum subsidence (> 4 km) occurred during the Early Cretaceous whereas rifting ended during the Middle Jurassic. The maximum burial recorded in the Bled Chetihat basin was attained during the late Oligocene with maximum thicknesses of almost 6.2 km. In the Tunisian Atlas (Gabés Basin), showing a maximum subsidence of 3.5 km, the tectonic subsidence displays a long-lasting and smooth curve up to present day. The highest rates of tectonic subsidence roughly coinciding with the Early-Late Cretaceous boundary, seems related to the Sirt rifting in Libya that also affected the eastern margin of Tunisia (Frizon de Lamotte, 2009 and references therein).

The diachronism between extension and diapirism compared to the subsidence curves may strongly indicate that peaks of fastest subsidence in Morocco and Algeria must be related to salt withdrawal from beneath the studied locations during diapirism stages. Although in Tunisia the rifting phase is longer and high subsidence rate peaks are partially coeval to the extension, diapirism cannot be ruled out as additional subsidence mechanism as would be suggested by the large amount of diapiric structures described for the area.

CONCLUSIONS

Twenty-seven new measurements of vitrinite reflectance data have been obtained in the central part of the Central High Atlas with values ranging from 0.81 to 1.98% for most of the samples, which show a good fit with their relative Lower Jurassic stratigraphic positions

in the Tazoult ridge and the Amezraï minibasin. High values up to 3.05% are calculated close to diapiric structures intruded by Upper Jurassic gabbro bodies.

Subsidence curves in the non-diapiric and marginal Djebel Bou Dahar platform and adjacent basin during Sinemurian and Pliensbachian periods show similar long-term and low-rate tectonic and total subsidence of around 0.06 and 0.08 mm yr^{-1}, respectively. The roughly parallel evolution of both total and tectonic subsidence curves indicates the tectonic influence in total subsidence of the platform-basin system, as corroborated by the syndepositional activity of outcropping normal faults.

Subsidence curves in the diapiric Tazoult salt wall and Amezraï minibasin reveal higher rates than in the Djebel Bou Dahar marginal carbonate platform. The SE flank of the Tazoult salt wall subsided tectonically at rates of 0.15 $mmyr^{-1}$ during the early Pliensbachian, decreasing to 0.01 $mmyr^{-1}$ through the late Pliensbachian-Toarcian and increasing again to 0.27 $mmyr^{-1}$ in Aalenian times. For the same periods of time, the total subsidence rates were 0.22, 0.09 and 0.74 $mmyr^{-1}$, respectively. Higher rates of tectonic subsidence characterise the sinking evolution of the Amezraï minibasin involving 0.17 $mmyr^{-1}$, 0.06 $mmyr^{-1}$ and 0.32 $mmyr^{-1}$, respectively, for the same periods of time as set forth in the Tazoult salt wall. The equivalent total subsidence rates were 0.38, 0.19 and 0.98 $mmyr^{-1}$, respectively. For the two first periods of time, the rates are two-fold their equivalent in the Tazoult salt wall.

Larger amounts of subsidence in the Tazoult salt wall and the Amezraï minibasin point to a combination of normal fault extension and salt withdrawal from beneath the minibasin as triggering mechanisms in front of the single normal fault extension for the non-

diapiric Djebel Bou Dahar marginal platform and basin domain where both tectonic and total subsidence rates were one order of magnitude smaller.

Numerous thermal models have been made to test alternative evolutions for both paleo heat flow estimations during rift and post-rift periods from which six are presented. All these models need extra burial to fit the reflectance of vitrinite curve ranging from 800 to 2400 m. In order to build geohistory plots we use in this work the model with paleo heat flow of 105 mW/m^2 from 189 to 140 Ma (Sinemurian-Pliensbachian to earliest Cretaceous) and post-rift paleo heat flow set at 60 mW/m^2 up to present day. For the chosen values, the needed extra burial is about 1200 m in the scenario with a roughly continuous sedimentation during Late Jurassic and Cretaceous times.

An alternative scenario with Late Jurassic-Early Cretaceous exhumation event has been proposed by other authors as a consequence of the widening of the West Moroccan Arch. We model this alternative scenario, which implies about 1.4 km of extra burial prior to the Late Jurassic-Early Cretaceous exhumation phase followed by around 1.6 km of extra burial preceding the Alpine inversion of the Atlas in order to reproduce the observed thermal maturation in the Tazoult-Amezraï region.

Subsidence curves from different localities of the Atlas Tethyan domain reveal that the fastest subsidence episodes and the maximum burials reached become younger from west to east. The comparisons among subsidence curves, timing of extension and salt diapirism evidence the close link between diapirism and high subsidence rate periods along the Tethyan domain of the Atlas system.

AKNOWLEDGEMENTS

This study was part of a collaborative research project funded by Statoil Research Centre, Bergen (Norway) and by the CSIC-FSE 2007-2013 JAE-Doc postdoctoral research contract (E.S.). The Spanish Ministry of Education and Science provided additional funding (MEC) through the projects Intramural Especial (CSIC 201330E030) and MITE (CGL 2014-59516). This research was supported by the Grup Consolidat de Recerca "Geologia Sedimentària" de la Generalitat de Catalunya (2014GSR251). We are grateful to Statoil for its support and permission to publish this study. Beicip-Franlab is also acknowledged for providing academic licenses of the GENEX® software, INCAR for the analysis of vitrine samples, and Marc Español for his technical support. The authors acknowledge the use of the Move Software Suite granted by Midland Valley's Academic Software Initiative. This paper benefited from the discussion on thermal modelling with Manel Fernandez and Ignacio Marzán from ICTJA-CSIC and by the constructive reviews from Dominique Frizon de Lamotte, Victoria Sachse and Editor Sébastien Castelltort.

CONFLICT OF INTEREST SECTION

No conflict of interest declared

REFERENCES

ALLEN, P.A. & ALLEN, J.R. (2005) *Basins Analysis. Principles & Applications*, 2nd edn. Blackwell Scientific Publications, Oxford.

ARBOLEYA, M.L., TEIXELL, A., CHARROUD, M. & JULIVERT, M. (2004) A Structural Transect through the High and Middle Atlas of Morocco. *Journal of African Earth Sciences*, **39,** 319-327.

BABAULT, J., TEIXELL, A., STRUTH, L., VAN DEN DRIESSCHE, J., ARBOLEYA, M.L. & TESÓN, E. (2013) Shortening, Structural Relief and Drainage Evolution in Inverted Rifts: Insights from the Atlas Mountains, the Eastern Cordillera of Colombia and the Pyrenees. *Geological Society, London, Special Publications*, **377**.

BALESTRIERI, M.L., MORATTI, G., BIGAZZI, G. & ALGOUTI, A. (2009) Neogene Exhumation of the Marrakech High Atlas (Morocco) Recorded by Apatite Fission-Track Analysis. *Terra Nova*, **21,** 75-82.

BARBERO, L., TEIXELL, A., ARBOLEYA, M.-L., RIO, P.D., REINERS, P.W. & BOUGADIR, B. (2007) Jurassic-to-Present Thermal History of the Central High Atlas (Morocco) Assessed by Low-Temperature Thermochronology. *Terra Nova*, **19,** 58-64.

BAUDON, C., FABUEL-PEREZ, I. & REDFERN, J. (2009) Structural Style and Evolution of a Late Triassic Rift Basin in the Central High Atlas, Morocco: Controls on Sediment Deposition. *Geological Journal*, **44,** 677-691.

BAUDON, C., REDFERN, J. & VAN DEN DRIESSCHE, J. (2012) Permo-Triassic Structural Evolution of the Argana Valley, Impact of the Atlantic Rifting in the High Atlas, Morocco. *Journal of African Earth Sciences*, **65,** 91-104.

BEAUCHAMP, W., ALLMENDINGER, R.W., BARAZANGI, M., DEMNATI, A., EL ALJI, M. & DAHMANI, M. (1999) Inversion Tectonics and the Evolution of the High Atlas Mountains, Morocco, Based on a Geological-Geophysical Transect. *Tectonics*, **18,** 163-184.

BOUCHOUATA, A. (1994) La Ride De Talmest-Tazoult (Haut Atlas Central Maroc), Lithostratigraphie, Biostratigraphie Et Relations Tectonique-Sédimentation Au Cours Du Jurassique. *Strata, série 2 (memoires)*, **25,** 219.

BOUCHOUATA, A., CANEROT, J., SOUHEL, A. & ALMERAS, Y. (1995) Jurassic Sequence Stratigraphy and Geodynamic Evolution in the Talmest-Tazoult Area, Central High Atlas, Morocco. *Comptes Rendus de l'Académie des Sciences*, **320,** 749-756.

BOUKADI, N. & BEDIR, M. (1996) Halokinesis in Tunisia: Tectonic Context and Chronology of Events. *Comptes Rendus de l'Academie de Sciences - Serie IIa: Sciences de la Terre et des Planetes*, **322,** 587-594.

BRACÈNE, R., PATRIAT, M., ELLOUZ, N. & GAULIER, J.-M. (2003) Subsidence History in Basins of Northern Algeria. *Sedimentary Geology*, **156,** 213-239.

BRECHBÜHLER, Y.A., BERNASCONI, R. & SCHAER, J.P. (1988) Jurassic Sediments of the Central High Atlas of Morocco: Deposition, Burial and Erosian History. In: *The Atlas System of Morocco* (Ed. by V. Jacobshagen), *Lecture Notes in Earth Sciences*, **15**, 201-217. Springer Berlin Heidelberg.

BREDE, R., HAUPTMANN, M. & HERBIG, H.G. (1992) Plate Tectonics and Intracratonic Mountain Ranges in Morocco - the Mesozoic-Cenozoic Development of the Central High Atlas and the Middle Atlas. *Geologische Rundschau*, **81,** 127-141.

CHARRIÈRE, A., IBOUH, H. & HADDOUMI, H. (2011) Central High Atlas from Beni Mellal to Imilchil. Notes et Memoires du Service Géologique du Maroc, 559, 109-164.

COUREL, L., AÏT SALEM, H., BENAOUISS, N., ET-TOUHAMI, M., FEKIRINE, B., OUJIDI, M., SOUSSI, M. & TOURANI, A. (2003) Mid-Triassic to Early Liassic Clastic/Evaporitic Deposits over the Maghreb Platform. *Palaeogeography, Palaeoclimatology, Palaeoecology*, **196,** 157-176.

DOMÈNECH, M., TEIXELL, A., BABAULT, J. & ARBOLEYA, M.L. (2014) The Inverted Triassic Rift of the Marrakech High Atlas: A Reappraisal of Basin Geometries and Faulting Histories. *Tectonophysics*.

DOMÈNECH, M. (2015) Rift Opening and Inversion in the Marrackech High Atlas: Integrated Structural and Thermochronologic Study. PHd. tHESIS Thesis, Universitat Autònoma de Barcelona, Bellaterra, Spain.

DU DRESNAY, R. (1976) Carte Géologique Du Marroc Huat Atlas D'anoual-Bou Anane (Haut Atlas Oriental). *Notes et Memoires du Service Géologique du Maroc (246)*.

DUPRE, S., BERTOTTI, G. & CLOETINGH, S. (2007) Tectonic History Along the South Gabon Basin: Anomalous Early Post-Rift Subsidence. Marine and Petroleum Geology, 24, 151-172.

ELLOUZ, N., PATRIAT, M., GAULIER, J.-M., BOUATMANI, R. & SABOUNJI, S. (2003) From Rifting to Alpine Inversion: Mesozoic and Cenozoic Subsidence History of Some Moroccan Basins. *Sedimentary Geology*, **156,** 185-212.

ETTAKI, M., IBOUH, H., CHELLAÏ, E.H. & MILHI, A. (2007) Liassic Diapiric Structures from the Central High Atlas, Morocco; Ikerzi Ride Example. *Africa Geoscience Review*, **14,** 79-93.

FADILE, A. (2003) Carte Géologique Du Marroc, Feuille Imilchil. *Notes et Memoires du Service Géologique du Maroc (397)*.

FRAISSINET, C., EL ZOUINE, M., MOREL, J.-L., POISSON, A., ANDRIEUX, J. & FAURE-MURET, A. (1988) Structural Evolution of the Southern and Northern Central High Atlas in Paleogene and Mio-Pliocene Times. In: *The Atlas System of Morocco* (Ed. by V. Jacobshagen), *Lecture Notes in Earth Sciences*, **15**, 273-291. Springer Berlin Heidelberg.

FRIZON DE LAMOTTE, D., BEZAR, B.S., BRACÈNE, R. & MERCIER, E. (2000) The Two Main Steps of the Atlas Building and Geodynamics of the Western Mediterranean. Tectonics, 19, 740-761.

FRIZON DE LAMOTTE, D., ZIZI, M., MISSENARD, Y., HAFID, M., AZZOUZI, M., MAURY, R.C., CHARRIÈRE, A., TAKI, Z., BENAMMI, M. & MICHARD, A. (2008) The Atlas System. In: *Continental Evolution: The Geology of Morocco* (Ed. by, 133-202.

FRIZON DE LAMOTTE, D., LETURMY, P., MISSENARD, Y., KHOMSI, S., RUIZ, G., SADDIQI, O., GUILLOCHEAU, F. & MICHARD, A. (2009) Mesozoic and Cenozoic Vertical Movements in the Atlas System (Algeria, Morocco, Tunisia): An Overview. *Tectonophysics*, **475,** 9-28.

FRIZON DE LAMOTTE, D., RAULIN, C., MOUCHOT, N., WROBEL-DAVEAU, J.-C., BLANPIED, C. & RINGENBACH, J.-C. (2011) The Southernmost Margin of the Tethys Realm During the Mesozoic and Cenozoic: Initial Geometry and Timing of the Inversion Processes. *Tectonics*, **30,** 1-22.

FRIZON DE LAMOTTE, D., FOURDAN, B., LELEU, S., LEPARMENTIER, F. & DE CLARENS, P. (2015) Style of Rifting and the Stages of Pangea Breakup. Tectonics, 34, 1009-1029.

GHORBAL, B., BERTOTTI, G., FOEKEN, J. & ANDRIESSEN, P. (2008) Unexpected Jurassic to Neogene Vertical Movements in 'Stable' Parts of Nw Africa Revealed by Low Temperature Geochronology. *Terra Nova*, **20,** 355-363.

GÖRLER, K., HELMDACH, F.-F., GAEMERS, P., HEIßIG, K., HINSCH, W., MÄDLER, K., SCHWARZHANS, W. & ZUCHT, M. (1988) The Uplift of the Central High Atlas as Deduced from Neogene Continental Sediments of the Ouarzazate Province, Morocco. In: *The Atlas System of Morocco* (Ed. by V. Jacobshagen), *Lecture Notes in Earth Sciences*, **15**, 359-404. Springer Berlin Heidelberg.

GOUIZA, M., BERTOTTI, G., HAFID, M. & CLOETINGH, S. (2010) Kinematic and Thermal Evolution of the Moroccan Rifted Continental Margin: Doukkala-High Atlas Transect. *Tectonics*, **29**.

GRADSTEIN, F.M., OGG, J.G., SCHMITZ, M.D. & OGG, G.M. (2012) *The Geologic Time Scale 2012*. Elsevier, Boston.

GRÉLAUD, C., RAZIN, P., JOUSSIAUME, R., MALAVAL, M., VERGÉS, J., SAURA, E., MARTÍN-MARTÍN, J.D., MORAGAS, M., HUNT, D. & MESSAGER, G. (2014) Diapiric Control on Jurassic Carbonate Systems of the High Atlas Basin, Morocco. *AAPG Annual Meeting*. Houston, Texas.

HADDOUMI, H., AIMERAS, Y., BODERGAT, A.-M., CHARRIERE, A., MANGOLD, C. & BENSHILI, K. (1998) Âges Et Environnements Des Couches Rouges D'anoual (Jurassique Moyen Et Crétacé Inférieur, Haut-Atlas Oriental, Maroc). *Comptes Rendus de l'Académie des Sciences - Series IIA - Earth and Planetary Science*, **327,** 127-133.

HADDOUMI, H., CHARRIÈRE, A., FEIST, M. & ANDREU, B. (2002) New Ages (Upper Hauterivian-Lower Barremian) of the Continental 'Red Beds' of the Moroccan Central High Atlas; Consequences on the Ages of the Magmatism and of the Mesozoic Tectonics of the Atlasic Belt. *Nouvelles datations (Hauterivien supérieur-Barrémien inférieur) dans les «Couches rouges» continentales du Haut Atlas central marocain ; conséquences sur l'âge du magmatisme et des structurations mésozoïques de la chaîne Atlasique*, **1,** 259-266.

HADDOUMI, H., CHARRIERE, A., ANDREU, B. & MOJON, P.-O. (2008) Les Dépôts Continentaux Du Jurassique Moyen Au Crétacé Inférieur Dans Le Haut Atlas Oriental (Maroc) : Paléoenvironnements Successifs Et Signification Paléogéographique. *Carnets de Geologie*, **CG2008,** 1-29.

HADDOUMI, H., CHARRIÈRE, A. & MOJON, P.O. (2010) Stratigraphy and Sedimentology of the Jurassic-Cretaceous Continental " Redbeds" of the Central High Atlas (Morocco): Paleogeographical and Geodynamical Implications. *Geobios*, **43,** 433-451.

HAFID, M. (2000) Triassic-Early Liassic Extensional Systems and Their Tertiary Inversion, Essaouira Basin (Morocco). *Marine and Petroleum Geology*, **17,** 409-429.

HAFID, M., TARI, G., BOUHADIOUI, D., MOUSSAID, I., ECHARFAOUI, H., SALEM, A., NAHIM, M. & DAKKI, M. (2008) Atlantic Basins. In: *Continental Evolution: The Geology of Morocco* (Ed. by, 303-329.

HODGSON, N.A., FARNSWORTH, J. & FRASER, A.J. (1992) Salt-Related Tectonics, Sedimentation and Hydrocarbon Plays in the Central Graben, North Sea, Ukcs. *Geological Society Special Publication*. **67,** 31-63.

HUDEC, M.R., JACKSON, M.P.A. & SCHULTZ-ELA, D.D. (2009) The Paradox of Minibasin Subsidence into Salt: Clues to the Evolution of Crustal Basins. *Geological Sociaty American Bulletin*, **121,** 201-221.

IBOUH, H., CHARRIÈRE, A. & MICHARD, A. (2011) Middle Jurassic Unsteady Sedimentation in the High Atlas Basin (Imilchil Area, Morocco) Controlled by Halokinetic and Regional Vertical Movements. *AAPG Search and Discovery*, **#90137**.

JOSSEN, J.A. & COUVREUR, G. (1990) Carte Géologique Du Marroc, Feuille Zawyat Ahançal. Notes et Memoires du Service Géologique du Maroc (355).

JOURDAN, F., MARZOLI, A., BERTRAND, H., CIRILLI, S., TANNER, L.H., KONTAK, D.J., MCHONE, G., RENNE, P.R. & BELLIENI, G. (2009) 40ar/39ar Ages of Camp in North America: Implications for the Triassic-Jurassic Boundary and the 40k Decay Constant Bias. *Lithos*, **110,** 167-180.

JOUSSIAUME, R., MALAVAL, M., RAZIN, P., GRELAUD, C., MESSAGER, G., MARTIN-MARTIN, J.D., SAURA, E., MORAGAS, M., VERGES, J. & HUNT, D. (2014). *Characterization of Syn-Diapiric Jurassic Sedimentation in the Taghia and Tazoult Areas, Central High Atlas, Morocco*. 19th International Sedimentological Congress, Geneva, Switzerland, International Association of Sedimentologist.

KENTER, J.A.M. & CAMPBELL, A.E. (1991) Sedimentation on a Lower Jurassic Carbonate Platform Flank: Geometry, Sediment Fabric and Related Depositional Structures (Djebel Bou Dahar, High Atlas, Morocco). *Sedimentary Geology*, **72,** 1-34.

LABAILS, C. & ROEST, W.R. (2010) Comment on 'Breakup of Pangaea and Plate Kinematics of the Central Atlantic and Atlas Regions' by Antonio Schettino and Eugenio Turco. *Geophysical Journal International*, **183,** 96-98.

LACHKAR, N., GUIRAUD, M., EL HARFI, A., DOMMERGUES, J.L., DERA, G. & DURLET, C. (2009) Early Jurassic Normal Faulting in a Carbonate Extensional Basin: Characterization of Tectonically Driven Platform Drowning (High Atlas Rift, Morocco). *Journal of the Geological Society*, **166,** 413-430.

LAVILLE, E. (1988) A Multiple Releasing and Restraining Stepover Model for the Jurassic Strike-Slip Basin of the Central High Atlas (Morocco). In: *Triassic-Jurassic Rifting: Continental Breakup and the Origin of the Atlantic Ocean and Passive Margind* (Ed. by W. Mainspeizer). Elsevier Science, New York.

LAVILLE, E. (2002) Role of the Atlas Mountains (Northwert Africa) Whithin the African-Eurasian Plate-Boundary Zone: Comment and Reply. *Geology*, **30,** 95-96.

LAVILLE, E., PIQUE, A., AMRHAR, M. & CHARROUD, M. (2004) A Restatement of the Mesozoic Atlasic Rifting (Morocco). *Journal of African Earth Sciences*, **38,** 145-153.

LE ROY, P., GUILLOCHEAU, F., PIQUÉ, A. & MORABET, A.M. (1998) Subsidence of the Atlantic Moroccan Margin During the Mesozoic. *Canadian Journal of Earth Sciences*, **35,** 476-493.

LE ROY, P. & PIQUÉ, A. (2001) Triassic-Liassic Western Moroccan Synrift Basins in Relation to the Central Atlantic Opening. *Marine Geology*, **172,** 359-381.

MAGRI, F., LITTKE, R., RODON, S., BAYER, U. & URAI, J.L. (2008) Temperature Fields, Petroleum Maturation and Fluid Flow in the Vicinity of Salt Domes. In: *Dynamic of Complex Intracontinental Basin: The Central European Basin System* (Ed. by R. Littke, U. Bayer, D. Gajewski & S. Nelskamp), 323 - 344. Springer.

MALAVAL, M., JOUSSIAUME, R., RAZIN, P., GRÉLAUD, C., MESSAGER, G., MARTÍN-MARTÍN, J.D., SAURA, E., MORAGAS, M., VERGÉS, J. & HUNT, D. (2014). *Characterization of Syn-Diapiric Jurassic Sedimentation in the Imilchil Area, Central High Atlas, Morocco*. 19th International Sedimentological Congress, Geneva, Switzerland, International Association of Sedimentologist.

MALUSÀ, M.G., POLINO, R., FERONI, A.C., ELLERO, A., OTTRIA, G., BAIDDER, L. & MUSUMECI, G. (2007) Post-Variscan Tectonics in Eastern Anti-Atlas (Morocco). *Terra Nova*, **19,** 481-489.

MERINO-TOMÉ, O., PORTA, G.D., KENTER, J.A.M., VERWER, K., HARRIS, P.M., ADAMS, E.W., PLAYTON, T. & CORROCHANO, D. (2012) Sequence Development in an Isolated Carbonate Platform (Lower Jurassic, Djebel Bou Dahar, High Atlas, Morocco): Influence of Tectonics, Eustacy and Carbonate Production. *Sedimentology*, **59,** 118-155.

MICHARD, A., IBOUH, H. & CHARRIÈRE, A. (2011) Syncline-Topped Anticlinal Ridges from the High Atlas: A Moroccan Conundrum, and Inspiring Structures from the Syrian Arc, Israel. *Terra Nova*, **23,** 314-323.

MILHI, A., ETTAKI, M., CHELLAI, E.H. & HADRI, M. (2002) The Lithostratigraphic Formations of Moroccan Jurassic Central High-Atlas: Interelationships and Paleogeographic Reconstitution. *Revue de Paleobiologie*, **21,** 241-256.

MISSENARD, Y., ZEYEN, H., FRIZON DE LAMOTTE, D., LETURMY, P., PETIT, C., SÉBRIER, M. & SADDIQI, O. (2006) Crustal Versus Asthenospheric Origin of Relief of the Atlas Mountains of Morocco. *Journal of Geophysical Research*, **111,** B03401, doi:03410.01029/02005JB003708.

MORGAN, P. (1983) Constraints on Rift Thermal Processes from Heat Flow and Uplift. Tectonophysics, 94, 277-298.

OUJIDI, M., COUREL, L., BENAOUISS, N., EL MOSTAINE, M., EL YOUSSI, M., ET TOUHAMI, M., OUARHACHE, D., SABAOUI, A. & TOURANI, A. (2000) Triassic Series of Morocco: Stratigraphy, Palaeogeography and Structuring of the Southwestern Peri-Tethyan Platform. An Overview. In: *Peri-Tethys Memoir 5: New Data on Peri-Tethyan*

Sedimentary Basins (Ed. by S. Crasquin-Soleau & E. Barrier), **182**, 23-38. Mémoires du Muséum National d´Histoire Naturelle, Paris.

OUKASSOU, M., SADDIQI, O., BARBARAND, J., SEBTI, S., BAIDDER, L. & MICHARD, A. (2013) Post-Variscan Exhumation of the Central Anti-Atlas (Morocco) Constrained by Zircon and Apatite Fission-Track Thermochronology. *Terra Nova*, **25,** 151-159.

PATRIAT, M., ELLOUZ, N., DEY, Z., GAULIER, J.M. & KILANI HATEN BEN, H. (2003) The Hammamet, Gabès and Chotts Basins (Tunisia): A Review of the Subsidence History. *Sedimentary Geology*, **156,** 241-262.

PERTHUISOT, V. (1981) Diapirism in Northern Tunisia. *Journal of Structural Geology*, **3,** 231-235.

PETERSEN, K. & LERCHE, I. (1996) Temperature Dependence of Thermal Anomalies near Evolving Salt Structures: Importance for Reducing Exploration Risk. *Geological Society, London, Special Publications*, **100,** 275-290.

PIERRE, A., DURLET, C., RAZIN, P. & CHELLAI, E.H. (2010) Spatial and Temporal Distribution of Ooids Along a Jurassic Carbonate Ramp: Amellago Outcrop Transect, High-Atlas, Morocco. **329,** 65-88.

POISSON, A., HADRI, M., MILHI, A., JULIEN, M. & ANDRIEUX, J. (1998) The Central High-Atlas (Morocco). Litho- and Chrono-Stratigraphic Correlations During Jurassic Times between Tinjdad and Tounfite. Origin of Subsidence. In: *Peri-Tethys Memoir 4: Epicratonic Basins of Peri-Tethyan Platforms* (Ed. by S. Crasquin & E. Barrier), **179**, 237-256. Mémoires du Muséum National d´Histoire Naturelle, Paris.

QUIQUEREZ, A., SARIH, S., ALLEMAND, P. & GARCIA, J.P. (2013) Fault Rate Controls on Carbonate Gravity-Flow Deposits of the Liassic of Central High Atlas (Morocco). *Marine and Petroleum Geology*, **43,** 349-369.

REDFERN, J., SHANNON, P.M., WILLIAMS, B.P.J., TYRRELL, S., LELEU, S., FABUEL PEREZ, I., BAUDON, C., ŠTOLFOVÁ, K., HODGETTS, D., VAN LANEN, X., SPEKSNIJDER, A., HAUGHTON, P.D.W. & DALY, J.S. (2010) An Integrated Study of Permo-Triassic Basins Along the North Atlantic Passive Margin: Implication for Future Exploration. *Geological Society, London, Petroleum Geology Conference series*, **7,** 921-936.

RIMI, A. (1990) Geothermal Gradients and Heat Flow Trends in Morocco. *Geothermics*, **19,** 443-454.

RIMI, A., FERNÁNDEZ, M., MANAR, A., MATSUSHIMA, J., OKUBO, Y., MOREL, J.-L., WINCKEL, A. & ZEYEN, H. (2005). *Geothermal Anomalies and Analysis of the Gravity, Fracturing and Magnetic Features in Morocco*. Proceedings World Geothermal Congress, Antalya, Turkey.

RUIZ, G.M.H., SEBTI, S., NEGRO, F., SADDIQI, O., FRIZON DE LAMOTTE, D., STOCKLI, D., FOEKEN, J., STUART, F., BARBARAND, J. & SCHAER, J.P. (2011) From Central Atlantic Continental Rift to Neogene Uplift - Western Anti-Atlas (Morocco). *Terra Nova*, **23,** 35-41.

SACHSE, V.F., LEYTHAEUSER, D., GROBE, A., RACHIDI, M. & LITTKE, R. (2012) Organic Geochemistry and Petrology of a Lower Jurassic (Pliensbachian) Petroleum Source Rock from Aït Moussa, Middle Atlas, Morocco. *Journal of Petroleum Geology*, **35,** 5-23.

SADDIQI, O., EL HAIMER, F.Z., MICHARD, A., BARBARAND, J., RUIZ, G.M.H., MANSOUR, E.M., LETURMY, P. & FRIZON DE LAMOTTE, D. (2009) Apatite Fission-Track Analyses on Basement Granites from South-Western Meseta, Morocco: Paleogeographic Implications and Interpretation of Aft Age Discrepancies. *Tectonophysics*, **475,** 29-37.

SAURA, E., VERGÉS, J., MARTÍN-MARTÍN, J.D., MESSAGER, G., MORAGAS, M., RAZIN, P., GRÉLAUD, C., JOUSSIAUME, R., MALAVAL, M. & HOMKE, S. (2014) Syn-to Post-Rift

Diapirism and Minibasins of the Central High Atlas (Morocco): The Changing Face of a Mountain Belt. *Journal of the Geological Society*, **171,** 97-105.

SNOKE, A.W., SCHAMEL, S. & KARASEK, R.M. (1988) Structural Evolution of Djebel Debadib Anticline: A Clue to the Regional Tectonic Style of the Tunisian Atlas. *Tectonics*, **7,** 497-516.

STECKLER, M.S. & WATTS, A.B. (1978) Subsidence of the Atlantic-Type Continental Margin Off New York. Earth and Planetary Science Letters, 41, 1-13.

SWEENEY, J.J. & BURNHAM, A.K. (1990) Evaluation of a Simple Model of Vitrinite Reflectance Based on Chemical Kinetics. *American Association of Petroleum Geologists Bulletin*, **74,** 1559-1570.

SWEENEY, J.J., TALUKDAR, S., BURNHAM, A. & VALLEJOS, C. (1990) Pyrolysis Kinetics Applied to Prediction of Oil Generation in the Maracaibo Basin, Venezuela. *Organic Geochemistry*, **16,** 189-196.

TARI, G. & JABOUR, H. (2013) Salt Tectonics Along the Atlantic Margin of Morocco. *Geological Society, London, Special Publications*, **369,** 337-353.

TEIXELL, A., ARBOLEYA, M.-L. & JULIVERT, M. (2003) Tectonic Shortening and Topography in the Central High Atlas (Morocco). *Tectonics*, **22,** doi:10.1029/2002TC001460, 002003.

TEIXELL, A., AYARZA, P., ZEYEN, H., FERNANDEZ, M. & ARBOLEYA, M.-L. (2005) Effects of Mantle Upwelling in a Compressional Setting: The Atlas Mountains of Morocco. *Terra Nova*, **17,** 456-461.

TESÓN, E., PUEYO, E.L., TEIXELL, A., BARNOLAS, A., AGUSTÍ, J. & FURIÓ, M. (2010) Magnetostratigraphy of the Ouarzazate Basin: Implications for the Timing of Deformation and Mountain Building in the High Atlas Mountains of Morocco. *Geodinamica Acta*, **23,** 151-165.

TESÒN, E. & TEIXELL, A. (2008) Sequence of Thrusting and Syntectonic Sedimentation in the Eastern Sub-Atlas Thrust Belt (Dadès and Mgoun Valleys, Morocco). *International Journal of Earth Sciences*, **97,** 103-113.

TURNER, P. & SHERIF, H. (2007) A Giant Late Triassic-Early Jurassic Evaporitic Basin on the Saharan Platform, North Africa. In: *Evaporites through Space and Time* (Ed. by B. C. Schreiber, S. Lugli & M. Babel), **285**, 87-105. Geological Society Special Publication.

VERWER, K., OSCAR, M.T., KENTER, J.A.M. & PORTA, G.D. (2009) Evolution of a High-Relief Carbonate Platform Slope Using 3d Digital Outcrop Models: Lower Jurassic Djebel Bou Dahar, High Atlas, Morocco. *Journal of Sedimentary Research*, **79,** 416-439.

WARME, J.E. (1988) Jurassic Carbonate Facies of the Central and Eastern High Atlas Rift, Morocco. In: *The Atlas System of Morocco* (Ed. by V. H. Jacobshagen), *Lecture Notes in Earth Sciences*, **15**, 169-199. Springer Berlin Heidelberg.

WILMSEN, M. & NEUWEILER, F. (2008) Biosedimentology of the Early Jurassic Post-Extinction Carbonate Depositional System, Central High Atlas Rift Basin, Morocco. *Sedimentology*, **55,** 773-807.

WILSON, R.C.L., HISCOTT, R.N., WILLIS, M.G. & GRADSTEIN, F.M. (1989) The Lusitanian Basin of West-Central Portugal: Mesozoic and Tertiary Tectonic, Stratigraphic, and Subsidence History. In: *Extensional Tectonics and Stratigraphy of the North Atlantic Margins, Aapg Memoir 46, Chapter 22* (Ed. by A. J. Tankard & H. R. Balkwill), 341-361.

XIE, X. & HELLER, P.L. (2009) Plate Tectonics and Basin Subsidence History. *Geological Society of America Bulletin*, **121,** 55-64.

ZEYEN, H., AYARZA, P., FERNÀNDEZ, M. & RIMI, A. (2005) Lithospheric Structure under the Western African-European Plate Boundary: A Transect across the Atlas Mountains and the Gulf of Cadiz. *Tectonics,* **24,** 1-16.

ZIZI, M. (1996) Triassic-Jurassic Extensional Systems and Their Neogene Reactivation in Northern Morocco (the Rides Pre-Rifaines and Guercif Basin). PhD Thesis, Rice University, Houston.

ZÜHLKE, R., BOUAOUDA, M.S., OUAJHAIN, B., BECHSTÄDT, T. & LEINFELDER, R. (2004) Quantitative Meso-/Cenozoic Development of the Eastern Central Atlantic Continental Shelf, Western High Atlas, Morocco. *Marine and Petroleum Geology*, **21,** 225-276.

TABLES

Table 1. List of stratigraphic units defined in the Djebel Bou Dahar area (Fig. 4) with their corresponding base and top ages (Merino-Tomé *et al.*, 2012), thicknesses, lithology percentages and bathymetry estimations.

Table 2 List of stratigraphic units defined in the Tazoult-Amezraï area with their corresponding base and top ages (Bouchouata *et al.*, 1995; Fadile, 2003), thicknesses, lithology percentages and bathymetry estimations, according to the interpreted sedimentary environment.

FIGURE LEGENDS

Fig. 1 Sketch map (Modified from Saura *et al.* 2014) showing the Atlas system extending from Morocco to Tunisia. Red box (Tazoult-Amezraï) and black box (Djebel Bou Dahar) show our study areas, and star symbols indicate the location of published subsidence studies.

Fig. 2 Paleogeographic map of the Central High Atlas basin for Late Pliensbachian-Toarcian times (based on Milhi *et al.*, 2002 and Pierre *et al*., 2010) including the locations of diapiric structures (coloured in pink). The location of these structures is based on Saura *et al*. (2014) and reference therein. Black symbols show the location of subsidence curves presented in this work.

Fig. 3 Chart showing the timing of the Atlas rift according to different authors. The shown timings span from the Atlantic margin (west) to the Tunisian Atlas (east). The time scale is according to Gradstein *et al.* (2012).

Fig. 4 a) Geological map and restored cross section (A'-A) from Djebel Bou Dahar platform modified after Merino-Tomé *et al.* (2012). The location of the studied stratigraphic sections is indicated in both images. b) Stratigraphic sections showing the outcropping succession in both locations. The basin section shows a very continuous sedimentary record whereas the platform section shows a distinct angular unconformity between sequences I-II and V. c) Field picture of the Djebel Bou Dahar area showing the geometry of the carbonate platform in the slope domain.

Fig. 5 a) Google Earth image of the Tazoult - Amezraï area overlain with simplified geological map of the Tazoult diapir and the Amezraï minibasin (modified after Saura *et al.*,2014), with the location of the collected vitrinite samples (colour dots) and detailed stratigraphic logs (roman numerals) carried out by Joussiaume *et al.* (2014) and Malaval *et al.*, (2014). b) Stratigraphic sections showing the succession outcropping in the studied area and the thickness variation from the Tazoult diapir flank to the centre of the Amezraï minibasin. Time scale according to Gradstein *et al.* (2012). c) Cross-section across the Amezraï area (A-A') with the projection in the stratigraphic position of the collected vitrinite samples. The thinning on the diapir flanks is well constrained and observed at outcrop, whereas thicknesses of units in the core of the minibasin are not well constrained and are

likely conservative. d) and e) interpreted field pictures showing halokinetic geometries and the upper part of the outcropping sedimentary succession, respectively.

Fig. 6 Summary of the Tazoult and Amezraï stratigraphic logs showing the position of the collected samples. Numbers correspond to vitrinite reflectance values (%) and associated standard deviation for each sample. Locations of samples are shown in Figure 5. The right-hand list shows vitrinite reflectance values of samples coming from other localities of the area. Star symbols mark the anomalous results interpreted to reflect proximity (i.e. < 200 m) to igneous bodies that intruded the diapiric structures (see location map in Fig. 5). The two sample pictures show the difference between a non-altered (GM 824) and altered sample (ES 797) due to magmatic intrusions.

Fig. 7 Plots of total and tectonic subsidence curves from Djebel Bou Dahar platform and basin sections (see location in Fig.4). Triassic rifting has not been modelled due to data being unavailable. Stratigraphic units according to logs in Fig. 4 projected on top of plots together with age of recorded normal fault activity (Merino-Tomé et al., 2012). The timing of normal faulting is considered in this study as the age range of the Lower Jurassic (phase 2) rifting. Time scale according to Gradstein et al. (2012).

Fig. 8 Plots of total and tectonic subsidence curves from Tazoult ridge (a) and Amezraï basin (b) sections (see location in Fig. 5). Triassic and very early Lower Jurassic subsidence evolution is not modelled due to the lack of data. Subsidence curves from early Bajocian times result from the data obtained in burial models. Stratigraphic units according to logs in Fig. 5 projected on top of plots. Time scale according to Gradstein *et al.* (2012).

Fig. 9 Sketch map (Modified from Saura *et al.* 2014) showing the Moroccan Atlas system. Red box (Tazoult-Amezraï) and black box (Djebel Bou Dahar) show our study areas, and star symbols indicate the location of published thermochronology studies. Thick discontinuous line shows the boundary of the West Moroccan Arch from Frizon de Lamotte *et al.* (2009).

Fig. 10. (Next page) Thermal model plots based on the present-day Amezraï stratigraphic section showing: calculated vitrinite reflectance profiles (IFPRo and Easy%Ro) resulting from a short period of high heat flow occurrence (from 189 to 182.7 Ma) with heat flow of 70 mW/m^2 (a), 105 mW/m^2 (b) and 120 mW/m^2 (c). Plots d), e) and f) correspond to models with a long period of high heat flow occurrence (from 189 to 140 Ma) with heat flow of 70 mW/m^2, 105 mW/m2 and 120 mW/m^2, respectively. Dashed curves correspond to models with no additional burial and solid lines correspond to models with additional burial. The burial required to fit curves with analysed samples is detailed in each plot, and have been applied with a homogeneous sedimentation from 169 Ma to 80 Ma. All models include a period of low thermal conditions of 60 mW/m^2.

Fig. 11. a) Thermal model for alternative scenario with Late Jurassic-Early Cretaceous exhumation showing calculated vitrinite reflectance profiles (IFPRo and Easy%Ro). The models assume: a) long high heat flow event of 105 mW/m^2 from 189 to 140 Ma resulting in 1600 m of extra burial during the early Upper Cretaceous; b) extra-long heat flow event of 105 mW/m^2 from 189 to 110 Ma resulting in 1200 m of extra burial.

Fig. 12 a) Burial history plot and temperature evolution for the Amezraï minibasin; b) Burial history plot and reflectance vitrinite isolines for the Amezraï minibasin. Blue band highlights the stratigraphic unit containing our vitrinite reflectance dataset (Aguerd-n'Tazoult Fm.). Grey line shows the path of the base of the Jbel Choucht-Aganane Fm. according to the Upper Jurassic-Lower Cretaceous uplift model. Time scale according to Gradstein *et al.* (2012).

Fig. 13 Comparison of total subsidence curve of Amezraï minibasin with subsidence curves from other localities in the Moroccan Atlas (Time scale according to Gradstein *et al.*, 2012). The map shows the subsidence rate through time for each plotted location.

Fig. 14 Interpretation of the Rich transect including four different faulted blocks and the location of the three sections used to perform the subsidence analysis in the area (modified from Lachkar *et al.*, 2009); plots show the average tectonic subsidence curve, including subsidence rates, from Boutazart, Foum Zabel and Guerss sections, respectively, presented by Lachkar *et al.* (2009) and the obtained tectonic subsidence curves from our study in the Djebel Bou Dahar area. Lower Jurassic rifting stages proposed by Lachkar *et al.* (2009) (early and climax stages) are plotted together with the timing of normal fault activity in DBD (Merino-Tomé *et al.*, 2012).

Fig. 15 Subsidence curves and tectonic stages from West High Atlas (Zühlke *et al.*, 2004), Central High Atlas (this study), Algeria (Bracène *et al.*, 2003) and Tunisia (Patriat *et al.*, 2003). Diapirism (pink bar) is associated with different stages. Amezraï minibasin total subsidence is compared with Bled Chetihat and Aït Chedri Tizgui curves, and the Amezraï tectonic curve is compared with the Gabés basin tectonic curve. The map shows the ages of the main peak of subsidence in each locality and the age of diapirism.

Djebel Bou Dahar	Age Base (Ma)	Age Top (Ma)	Thicknesses (m)	Lithology (%)						Sedimentary Environment	Bathymetry (m)
				Sand	Silt	Shale	Limestone	Marls	Dolostone		
Basin section											
Aalenian	172,2	170	100	---	---	---	90	10	---	?	520
Toarcian	182,2	172,2	119	---	---	43	7	50	---	Basin	610
Drowning	183,2	182,2	0	---	---	---	---	---	---	Drowning	715
Sequence VI	186	183,2	57	---	---	---	58	42	---	Basin	500
Sequence V	187,3	186	18,5	---	---	---	65	35	---	Basin	430
Sequence IV	190,8	187,3	37,3	---	---	---	79	21	---	Basin	210
Sequence III	195,3	190,8	76,2	---	---	---	99	1	---	Distal ramp	0
Sequence I and II	200,5	195,3	226,7	---	---	1	65	2	32	Lagoon to intertidal	0
Platform section											
Aalenian	172,2	170	35	---	---	---	90	10	---	?	100
Toarcian	182,2	172,2	0,5	---	---	43	7	50	---	Condense level	100
Drowning	183,2	182,2	0	---	---	---	---	---	---	Drowning	100
Sequence VI*	186	183,2	134,7	---	---	---	39	---	---	Supratidal to lagoon	0
Sequence V*	187,3	186	55,3	---	---	---	90	---	---	Supratidal to lagoon	0
Erosion	195,3	187,3	-111	---	---	---	---	---	---	Supratidal	< 0
Sequence I and II*	200,5	195,3	226,6	---	---	1	64	1	32	Supratidal to lagoon	0
* remnant % corresponds to early cemented lithologies											

Amezraï area	Age Base (Ma)	Age Top (Ma)	Thicknesses (m)	Lithology (%)						Sedimentary Environment	Bathymetry (m)
				Sand	Silt	Shale	Limestone	Marls	Dolostone		
Tazoult ridge section											
Bin el Ouidane 3	169.6	169	---	---	---	---	50	50	---	Intertidal	15
Bin el Ouidane 2	170	169.6	---	---	---	---	40	60	---	Intertidal	15
Bin el Ouidane 1	170.7	170	690	---	5	5	75	15	---	Shallow platform	30
Aguerd n'Tazoult	171.1	170.7	176	---	5	---	65	30	---	Supratidal to intertidal	10
Hiatus	175	171.1	---	10	10	---	40	40	---	Intertidal to subtidal	20
Amezraï	185	175	775	15	15	25	25	20	---	Supratidal to intertidal	10
Jbel Choucht / Aganane	189	185	470	---	---	5	70	25	---	Lagoon & Shallow Platform	30
Bou Imoura	195.3	189	---	----	----	----	80	20	---	Shallow platform	30
Aït Bou Oulli	201.3	195.3	---	---	---	10	20	---	70	Supratidal	0
Amezraï section											
Bin el Ouidane 3	169.6	169	---	---	---	---	50	50	---	Intertidal	15
Bin el Ouidane 2	170	169.6	---	---	---	---	40	60	---	Intertidal	15
Bin el Ouidane 1	170.7	170	693.8	---	5	5	75	15	---	Shallow platform	30
Aguerd n'Tazoult	172.2	170.7	713.2	---	5	---	65	30	---	Supratidal to intertidal	10
Tafraout	174.5	172.2	256.8	10	10	---	40	40	---	Intertidal to subtidal	20
Amezraï	185	174.5	1748.9	15	15	25	25	20	---	Supratidal to intertidal	10
Jbel Choucht / Aganane	189	185	906.9	---	---	5	70	25	---	Lagoon & Shallow Platform	30
Bou Imoura	195.3	189	---	----	----	----	80	20	---	Shallow platform	30
Aït Bou Oulli	201.3	195.3	---	---	---	10	20	---	70	Supratidal	0

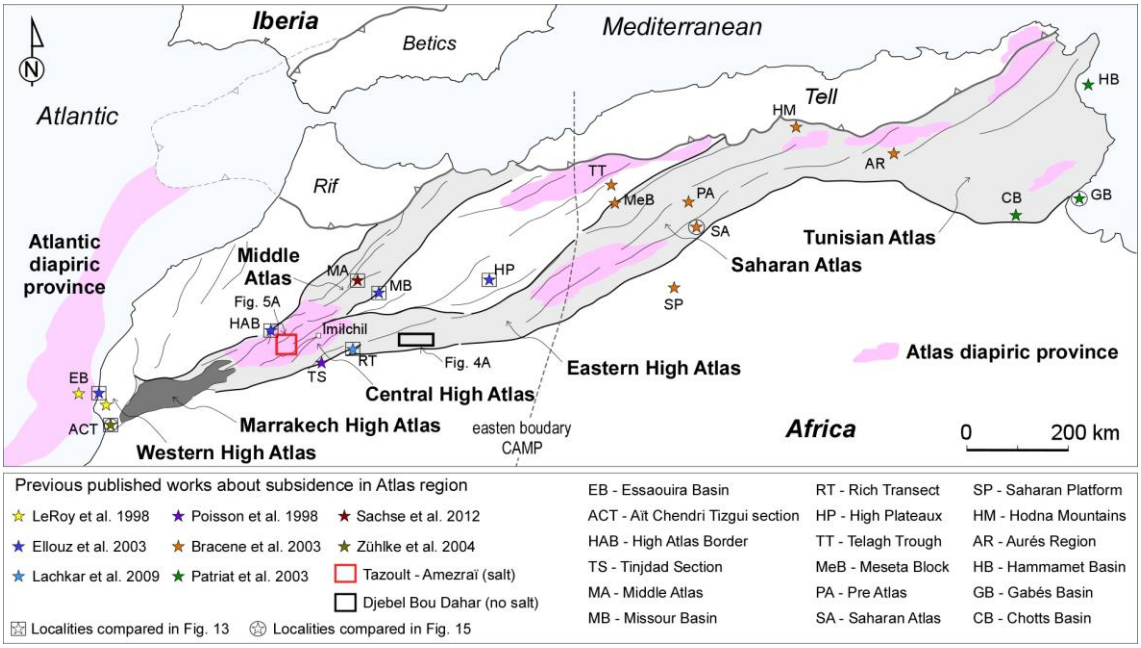

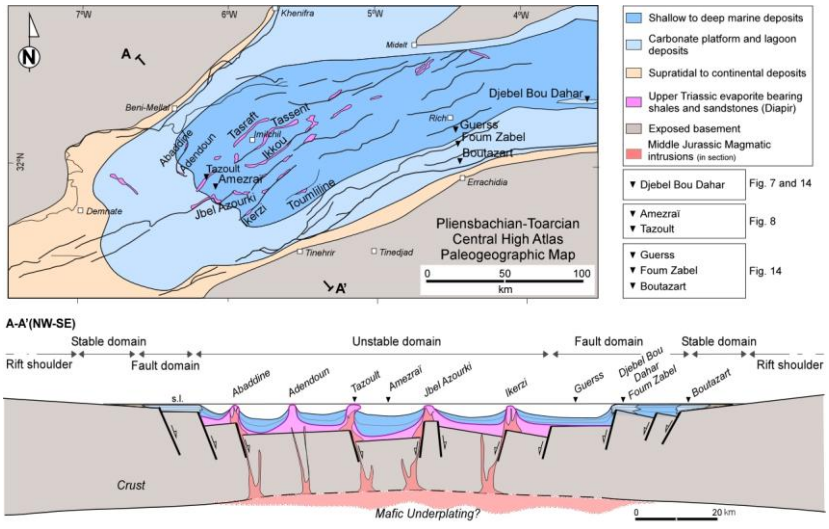

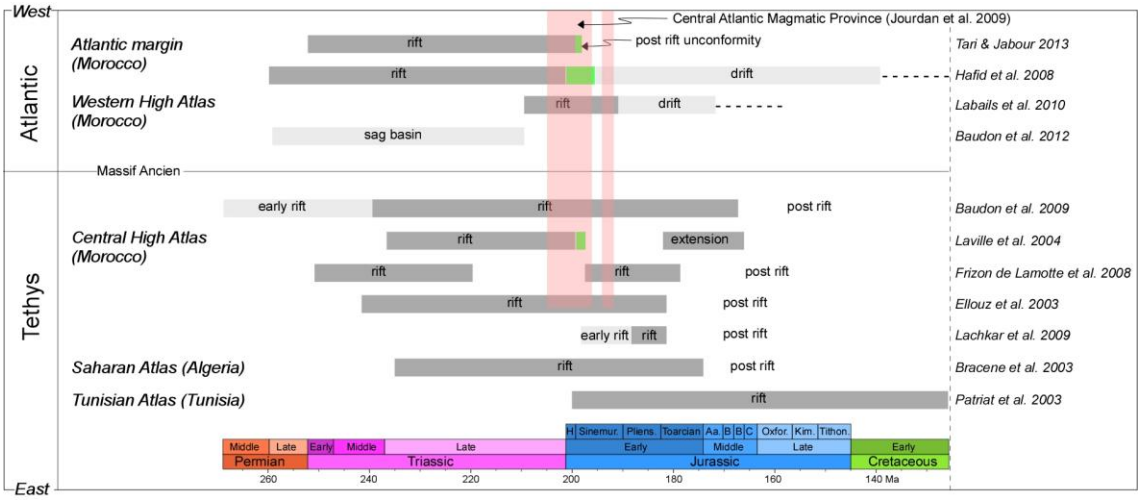

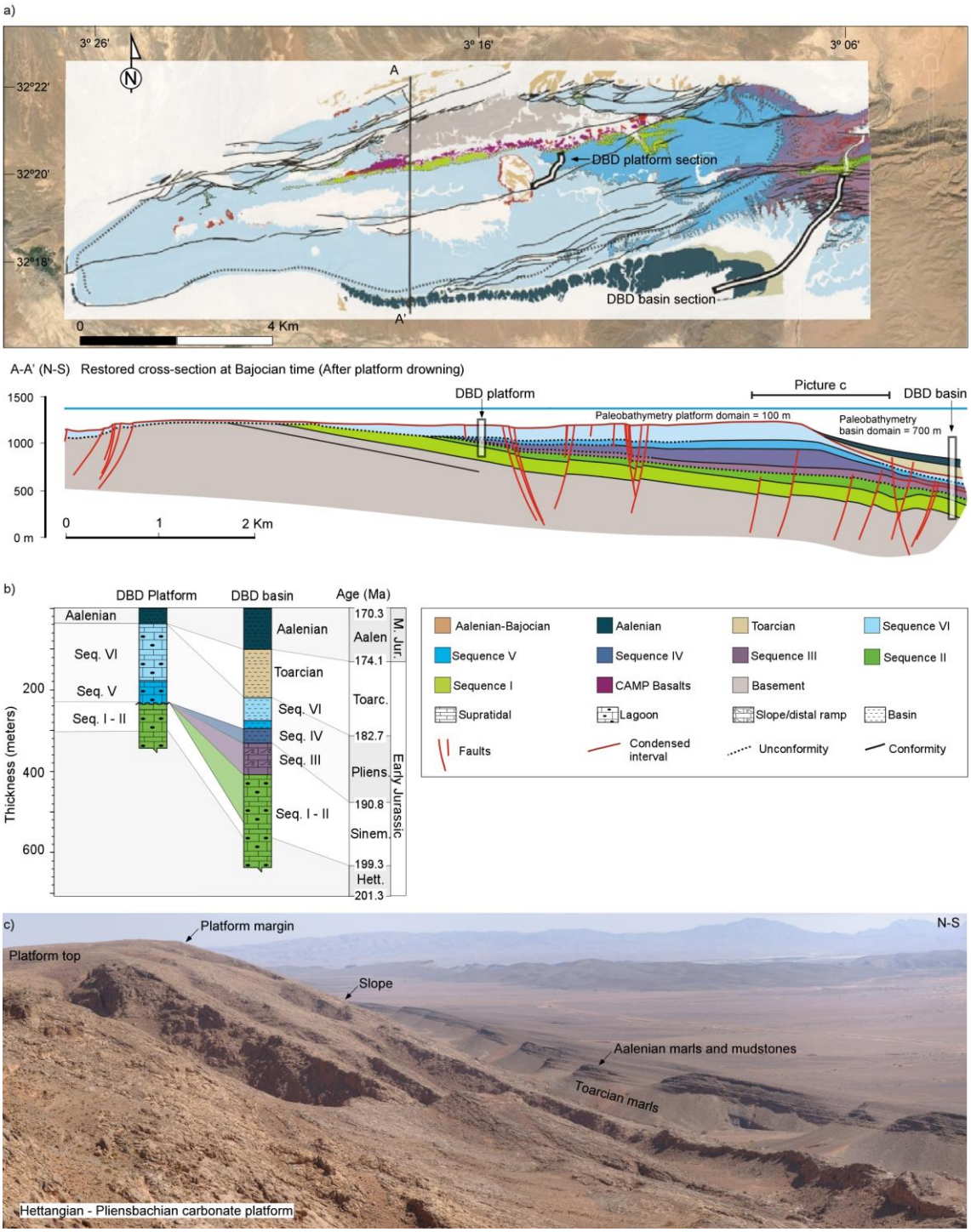

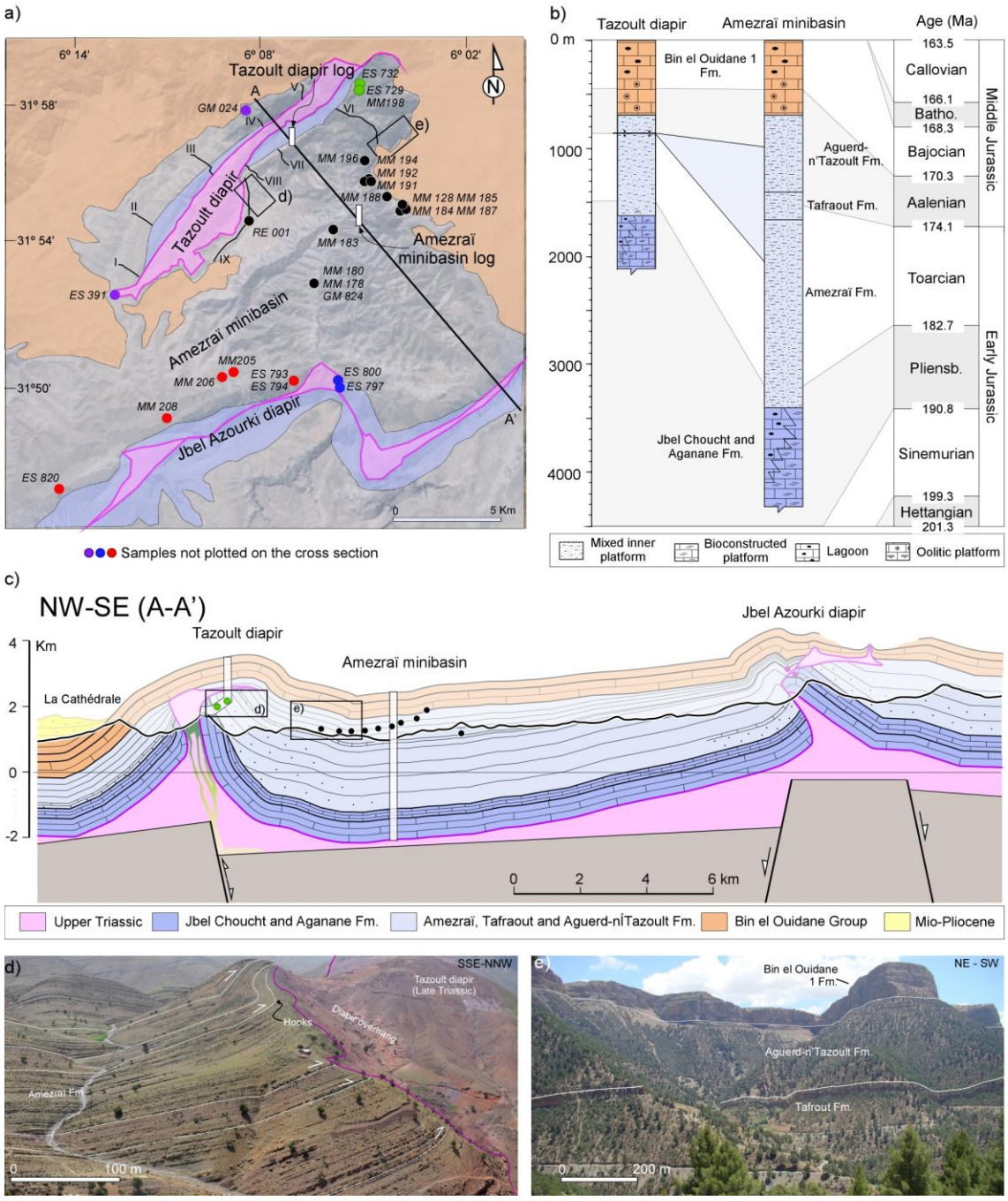

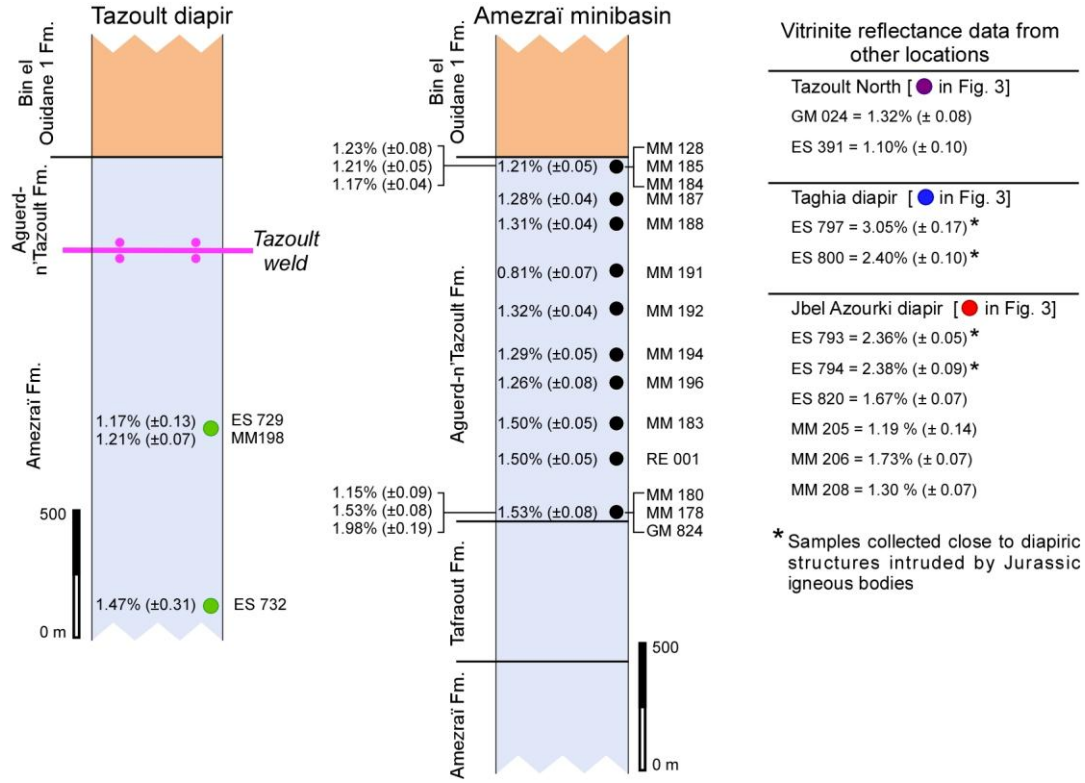

Sample GM 824

Sample ES 797 *